

Connections of Primary Auditory Cortex in the New World Monkey, *Saguinus*

L.E. LUETHKE, L.A. KRUBITZER, AND J.H. KAAS

Department of Hearing and Speech Sciences (L.E.L.) and Department of Psychology (L.A.K., J.H.K.), Vanderbilt University, Nashville, Tennessee 37240

ABSTRACT

Connections of primary auditory cortex (A-I) were investigated in the tamarin (*Saguinus fuscicollis*), a New World monkey. In each case, A-I was defined by multiunit recordings, and best frequencies were determined for neurons at different recording sites. Microlesions were placed to mark recording sites for correlation with cortical architecture. Following mapping, separate injections of up to three different tracers (HRP-WGA and fluorescent dyes) were placed into the representations of different frequencies within A-I. The results support several conclusions: (1) high to low frequencies are represented in a dorsocaudal to ventrorostral sequence in A-I, (2) intrinsic connections in A-I are more pronounced along isofrequency contours, (3) the pattern of connections between A-I and adjoining cortex suggests that this surrounding auditory cortex contains at least two tonotopically organized fields and possibly one or more additional auditory fields, (4) callosal connections of A-I are largely between parts of A-I matched for frequency representation, (5) thalamic connections of A-I include topographic connections with the ventral division of the medial geniculate complex (MGv) and more diffuse connections with the medial (MGm) and dorsal (MGd) divisions of the medial geniculate complex and the supragenicular nucleus (Sg), and (6) A-I projects bilaterally to the dorsal cortex of the inferior colliculus.

Key words: medial geniculate complex, inferior colliculus, callosal connections

The auditory cortex of monkeys clearly contains several fields, but only two have been well defined. One is the primary field, A-I, which has a systematic representation of tones from high to low in a caudomedial to rostralateral direction, as demonstrated with microelectrode mapping methods in macaque monkeys (Merzenich and Brugge, '73), owl monkeys (Imig et al., '77), and marmosets (Aitkin et al., '86). In these studies, A-I corresponds to a cytoarchitectonic field that is characterized by densely packed small cells in the granular and supragranular layers, auditory koniocortex. A second systematic representation of the audible frequency spectrum in auditory cortex has been demonstrated in most detail in owl monkeys (Imig et al., '77) and less fully in macaque monkeys (Merzenich and Brugge, '73). This field, termed rostralateral (RL) in macaque monkeys and rostral (R) in owl monkeys, adjoins the rostral border of A-I and contains a representation of tone frequencies from low to high in a caudorostral direction in macaque monkeys, and from high to low in a caudomedial to rostralateral direction in owl monkeys.

The frequency representation in RL appears to approximate a mirror image of that seen in A-I, reversing at the common low frequency border in macaque monkeys (Merzenich and Brugge, '73). However, in the owl monkey the frequency representation in R appears to be organized in a similar manner as A-I (Imig et al., '77). Despite this apparent difference in the tonotopic organization of R and RL, they are considered homologous because of their locations relative to A-I and their cytoarchitectonic similarities (Imig et al., '77; Brugge, '82). Whereas R resembles A-I in architectonic appearance, and A-I and R may have been combined in some architectonic studies, R has somewhat less dense

Accepted March 30, 1989.

Address reprint requests to Jon H. Kaas, Department of Psychology, Vanderbilt University, 301 Psychology Bldg., Nashville, TN 37240.

L.E. Luethke (Huerta) is presently at Ear, Nose and Throat Associates of Waterbury, 171 Grandview Avenue, Waterbury, CT 06708.

cell packing than A-I so that an architectonic distinction is possible (e.g., Merzenich and Brugge, '73; Imig et al., '77).

Other cortex around A-I has been described as responsive to auditory stimuli in macaque monkeys (Merzenich and Brugge, '73), owl monkeys (Imig et al., '77), galagos (Brugge, '82), and marmosets (Aitkin et al., '86), but responsiveness to auditory stimuli was reported as being generally reduced, and best frequencies were difficult to determine. However, the results from these limited recordings, together with architectonic data, have been used to postulate the existence of several surrounding auditory fields named by location relative to A-I (Merzenich and Brugge, '73; Imig et al., '77). In addition, injections of anatomical tracers in A-I or R of owl monkeys (FitzPatrick and Imig, '80) and A-I of marmosets (Aitkin et al., '88) have revealed interconnections between A-I and R and connections with auditory cortex surrounding A-I and R.

We addressed the question of cortical organization in these surrounding fields by injecting one to three different tracers into electrophysiologically identified frequency representations in A-I of tamarins. The resulting patterns of connections in flattened cortex support the view that several tonotopically organized fields border A-I and R. In addition, surface view patterns of intrinsic connections were found to be preferentially distributed along isofrequency contours in A-I, a pattern previously described in cats (Reale et al., '83; Matsubara and Phillips, '88).

The results also provided information on the nature of callosal and subcortical connections of A-I. In owl monkeys (FitzPatrick and Imig, '80) and marmosets (Aitkin et al., '88), A-I projects densely to A-I of the opposite hemisphere in what appears to be the homotopic location. Thus there is evidence that neurons with similar best frequencies in the two hemispheres are preferentially interconnected. We tested this assumption directly in some of our experiments by injecting tracers into known locations in the frequency map in A-I of one hemisphere, and later determined the frequency map of A-I of the other hemisphere. Thus transported label from a known frequency location in A-I of one hemisphere could be related to a frequency map of A-I in the other hemisphere.

The subcortical connections of A-I have been extensively described in cats (see Imig and Morel, '83 for review), but in primates there have been only two studies where connections were determined for sites clearly confined to A-I. In owl monkeys, A-I was shown to project to two subdivisions of the medial geniculate complex, MG_v and MG_m , and to the dorsal portion of the inferior colliculus (FitzPatrick and Imig, '78). In a more recent study in marmosets (Aitkin et al., '88), the medial geniculate complex was not subdivided, but evidence was presented for reciprocal connections with at least dorsal and ventral aspects of the complex. In addition, connections of A-I with the ventral portion of the medial geniculate complex were shown to be topographically organized. By using both fiber and Nissl preparations to study thalamic and collicular architecture, and by placing up to three tracers in known locations in A-I of tamarins, we obtained a more detailed description of the subcortical projection patterns of A-I in monkeys.

Tamarins were used in the present study because they are members of the family *Callitrichidae* (marmosets), which have a shallow lateral sulcus and a primary auditory area that is partly exposed on the surface of the temporal lobe. A-I has been mapped (Aitkin et al., '86) and connections studied (Aitkin et al., '88) in another member of the family,

the common marmoset (*Callithrix jacchus*). Preliminary reports of some of the present results have been published elsewhere (Luethke et al., '87).

METHODS

Microelectrode multiunit recordings were used to identify and define the borders of primary auditory cortex (A-I) in five adult tamarins (*Saguinus fuscicollis*). In the same animals, both cortical and subcortical connections were demonstrated by placing single injections of up to three anatomical tracers in different frequency representations within A-I. The physiological and anatomical results were subsequently related to cortical myeloarchitecture in brain sections cut parallel to the artificially flattened cortical surface. The patterns of subcortical connections were related to cytoarchitecture in sections cut in the frontal plane. In general, the microelectrode recording techniques and the anatomical procedures correspond to those outlined in Luethke et al. ('88).

Surgery

In all experiments sterile surgical procedures were followed. At the beginning of each experiment, animals were anesthetized with ketamine hydrochloride (50 mg/kg) supplemented with acepromazine maleate (1 mg/kg). Xylocaine hydrochloride, a local anesthetic, was injected subcutaneously along the incision line on the scalp. Supplemental doses of ketamine were given as needed to maintain a surgical level of anesthesia (see White et al., '82). Following anesthetization, skin on the dorsal aspect of the head was incised and retracted, the skull overlying the parietal-temporal cortex was removed, and the dura was retracted. An acrylic chamber was sealed around the craniotomy and filled with warm silicone fluid to prevent desiccation of the cortex. The exposed cortex was then photographed so that the blood vessel pattern could be used to mark the locations of electrode penetrations during the experiment. Finally, the electrode holder was positioned to orient the electrode perpendicular to the cortical surface.

Recording

Low-impedance tungsten microelectrodes (0.9–1.2 M Ω at 1 kHz) with tip exposures designed to record from small clusters of neurons were used for the recordings. The electrodes were advanced with an hydraulic microdrive and the recording depths were noted. Typical recording depths for auditory responses were 700–1,000 μ m from the pial surface. Several electrode penetrations were extended into the lower bank of the lateral sulcus and neural responses were determined at 200- μ m intervals. Lesions were made at points where marked changes in responsiveness were noted.

A Krohn-Hite oscillator was used to produce varying frequencies and intensities of pure tone stimuli. A model EXP-1 amplifier (Winston Electronics) allowed the intensities of audio signals to be preadjusted to provide a flat intensity output for frequencies from approximately 2 kHz to 30 kHz. An electronic switch was used to shape stimuli to have a rise-fall time of 6 msec and a duration of 200 msec. Stimuli were delivered to the animal at a rate of approximately one per second via hollow ear tubes coupled to audiometric drivers. The outputs of the audiometric drivers were calibrated before the experiments with a one-half-inch condenser mi-

A-I CONNECTIONS IN MONKEYS

crophone coupled to a one-third octave-band filter and sound level meter.

To obtain best frequencies for neurons in a given penetration, stimulus frequency and intensity were varied until a threshold (just noticeable) response was obtained. The neuronal responses were conventionally amplified, filtered, and displayed. Since stimulation of the contralateral ear resulted in strong responses and since stimulating both ears or the ipsilateral ear alone did not seem to affect estimates of best frequency, stimuli were typically presented to the contralateral ear (also see Merzenich and Brugge, '73). The tonotopic organization of A-I was determined by obtaining the best frequencies for a number of closely spaced recording sites. For some penetrations, neurons were stimulated by auditory clicks produced by tapping two metal rods together.

Injections

After recording, small electrolytic lesions were made at the borders of A-I or at other recording sites for later correlation of physiology and myeloarchitecture. For tamarins 87-22 and 87-29, single injections of each of three tracers [0.05–0.1 μ l of 0.1% horseradish peroxidase conjugated to wheat germ agglutinin (WGA-HRP), plus two of the following: 0.2–0.5 μ l of 1–3% fast blue, rhodamine, or diamidino yellow in 0.9% saline] were placed in different frequency representations within A-I. Calibrated glass micropipettes with tip diameters of 10–50 μ m were used to make the injections of WGA-HRP and Hamilton syringes were used for the fluorescent dyes. Following the injections, the skull opening was covered with an acrylic cap, the skin was sutured, and the animals were allowed to recover from anesthesia; 4 to 5 days later, these tamarins were deeply anesthetized and perfused. In addition, the contralateral primary auditory area in tamarins 87-44 and 87-45 was mapped immediately before perfusion so that callosal connections could be related to physiological data. To better define the intrinsic connections of A-I, HRP-WGA was the only tracer injected in tamarin 87-60. This animal had a postinjection survival of 2 days.

Histology and data analysis

Following their respective survival times, each animal was given a lethal dose of sodium pentobarbital and perfused through the heart with 0.9% saline followed by 2% paraformaldehyde in phosphate buffer (pH 7.4). The cerebral cortex was dissected from the rest of the brain, cut along the lateral fissure and within the temporal, occipital and frontal lobes, and "unfolded" to form a single flattened sheet (see Gould and Kaas, '81; Luethke et al., '88). The cortical hemispheres were flattened between glass plates and soaked in 30% sucrose phosphate buffer for 15–18 hours. The flattened cortical hemispheres were frozen and 40- μ m sections were cut parallel to the cortical surface. Alternate sections were processed with tetramethylbenzidine (see Mesulam, '78) to reveal transported HRP, mounted for fluorescent microscopy or stained for myelin with the Gallyas ('79) silver procedure. The thalamus and brainstem were cut in the frontal plane and alternate sections were processed with tetramethylbenzidine to reveal transported HRP, mounted for fluorescent microscopy, stained for cells with cresyl violet, stained for myelin, or reacted to reveal cytochrome oxidase activity (Wong-Riley, '79).

Detailed enlarged projection drawings were made of cortical sections to show injection sites, anterogradely labeled

axon terminals (from HRP-WGA injections only), retrogradely labeled cells (from all injections), and electrolytic lesions. Myelin-stained sections were drawn to show architectonic boundaries and electrolytic lesions. Drawings of individual sections of cortex were then aligned by using blood vessels, tissue artifacts, and electrolytic lesions to form one comprehensive reconstruction. These reconstructions indicated the locations of electrolytic lesions (which marked the physiologically defined borders of A-I), the extents of the injection sites, the distributions of transported tracers, and the architectonic boundaries for each case. Similarly, detailed enlarged projection drawings were made of thalamic and brainstem sections to form reconstructions that demonstrated the distribution of transported tracers and the cytoarchitectonic borders of thalamic and brainstem nuclei.

Characteristics of the tracers

The interpretation of data in the present study depends on estimates of the sizes of the uptake zones of the tracers. The blackened region in Figures 2, 5, 6, and 8 marks the zone of dense, uniform HRP-WGA label around the injection track. This zone corresponds to what has been called the "virtual" injection site by Shook et al. ('84). By comparing electrophysiological and anatomical data in the same animals, Shook et al. ('84) concluded that the effective uptake zone approximately corresponds to the central half of the virtual injection site. The effective uptake zones of diamidino yellow and fast blue appear to be limited to the region mechanically damaged by the injection syringe (Conde, '87). Although effective uptake zones have not been as rigorously studied for rhodamine, comparison of our data with other studies with this tracer (e.g., Thanos and Bonhoeffer, '83, '84; Thanos et al., '87) suggests that the effective injection uptake zone for rhodamine also is limited to or near the site of injection damage. Thus the injection zones of dense local label indicated in the present study are likely to include all of the effective uptake zones.

The various tracers differed in sensitivity and transport properties. The HRP-WGA was transported bidirectionally, whereas only retrograde transport was obvious for the fluorescent tracers. In each of the four tamarins with injections of three different tracers (HRP-WGA, plus two of the following: fast blue, rhodamine, and diamidino yellow), the HRP-WGA injection site was always the largest of the three, the fast blue injection site was smaller, and rhodamine and diamidino yellow injections always produced the smallest injection sites (e.g., see Figs. 5, 6, 8). Furthermore, the extents of the demonstrated connections (both cortical and subcortical) appeared to be proportional to the extents of the injection sites (e.g., see Figs. 5, 6, 10, 12). Thus the HRP-WGA revealed more widespread connections than did the fluorescent tracers. Undoubtedly, this was in part a result of survival times that were optimal for HRP-WGA but short for fluorescent tracers. Sometimes a particular fluorescent tracer was not effectively transported to some structures that exhibited labeling with the other tracers. For example, contralateral cortex never contained retrogradely transported fluorescent tracers, even though the transported HRP-WGA in contralateral A-I was usually quite dense (e.g., see Fig. 7). Other examples of differences in effectiveness of particular tracers are specified in Results.

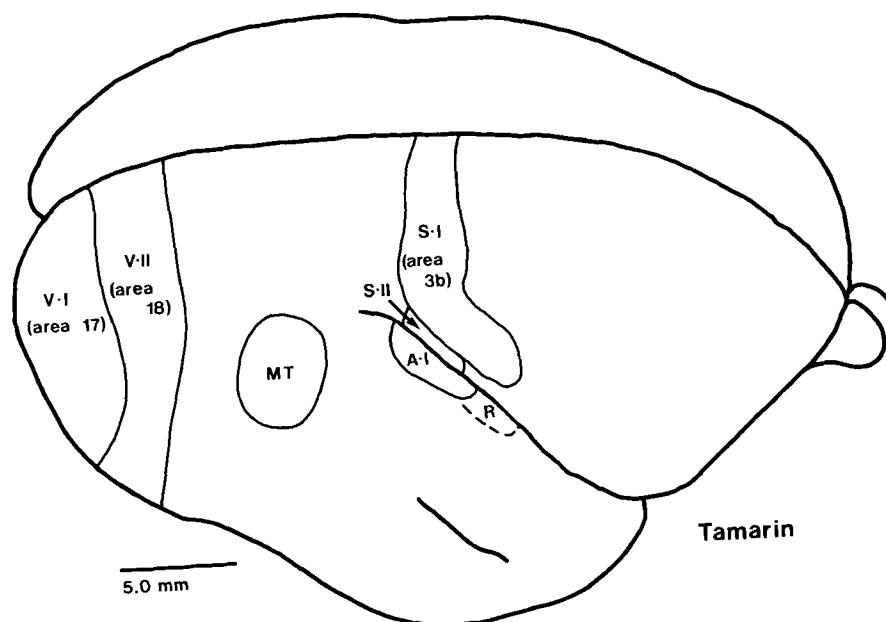


Fig. 1. The locations of auditory, visual, and somatosensory fields on a dorsolateral view of the brain of a tamarin. A-I, primary auditory cortex; MT, middle temporal visual area; R, rostral auditory area; S-I (area 3b), primary somatosensory area; S-II, second somatosensory area; V-I (area 17), primary visual area; V-II (area 18), second visual area.

RESULTS

Microelectrode multiunit recordings were used to determine the best frequencies for recording sites in A-I. The electrophysiological results guided the placement of as many as three different anatomical tracers into different frequency regions of A-I to reveal patterns of cortical and subcortical connections. The electrophysiological and connective data were then related to cortical myeloarchitecture and subcortical cytoarchitecture and differential staining for cytochrome oxidase activity.

Physiological and architectonic features of A-I and surrounding cortex

The primary auditory field, A-I, was identified by responsiveness to pure tones, a characteristic representation of tone frequencies, and dense myelination. Although a portion of the primary auditory cortex (A-I) is buried on the ventral bank of the lateral fissure, the majority of A-I extends onto the cortical surface of the temporal lobe (Figs. 1, 2).

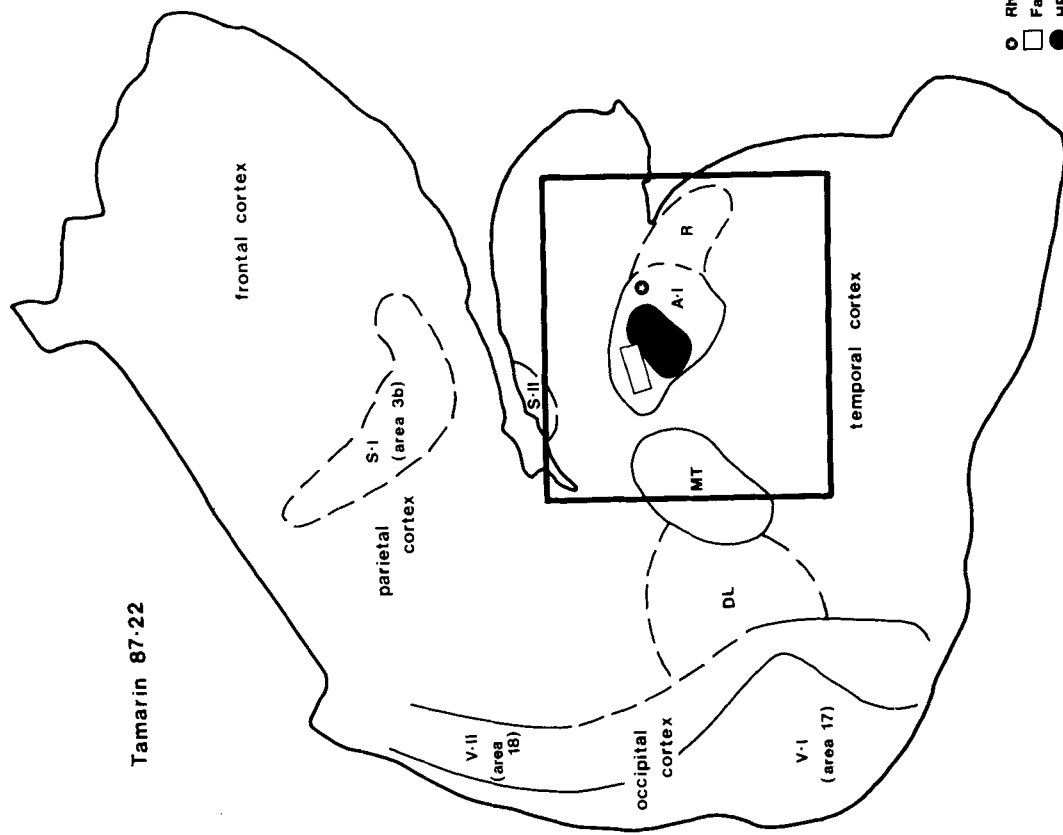
Responsiveness and tonotopic organization. During the recording sessions, our goal was to obtain enough physiological information about A-I to guide the placement of injections, rather than to obtain complete tonotopic maps. Nevertheless, the physiological results confirm and extend an understanding of the organization of auditory cortex.

Recordings from neurons in A-I were obtained from seven cortical hemispheres in five tamarins. Neurons in A-I were highly responsive to auditory stimuli, including clicks and pure tones. Repeating stimuli at rates of up to several times per second or for extended periods of time (up to several minutes) did not result in notable reductions in response

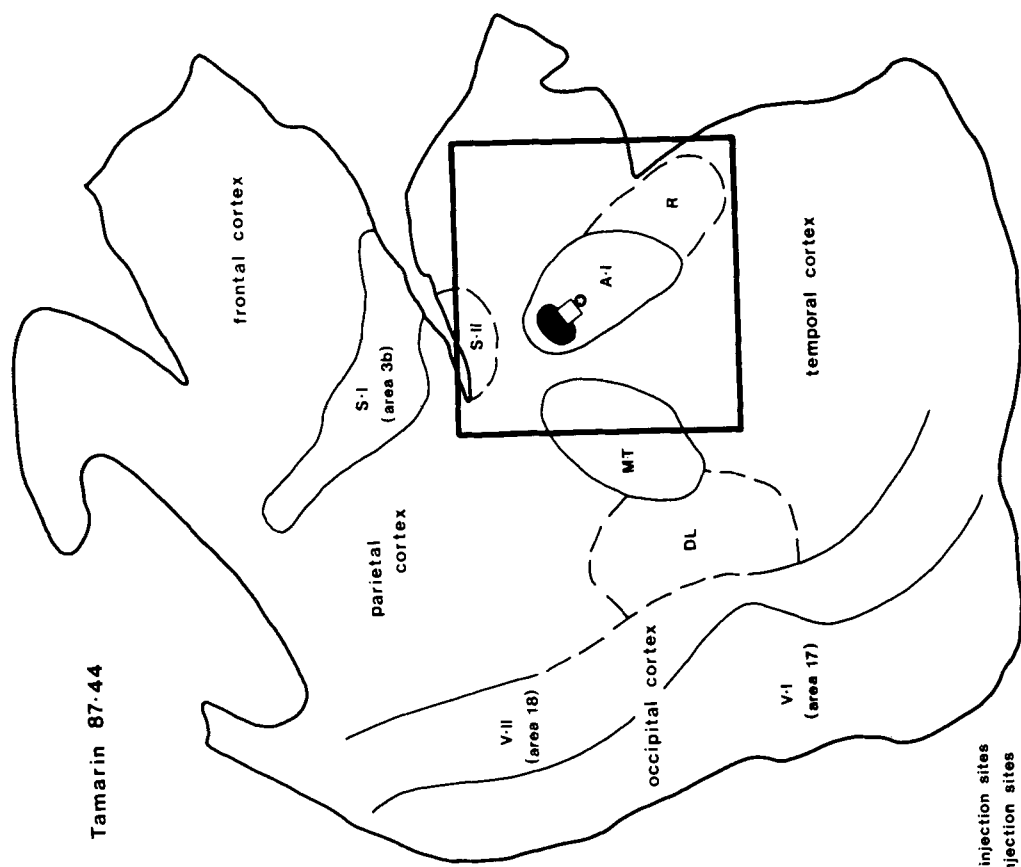
magnitude. Usually, best frequencies were easily determined by reducing tone intensities until responses were obtained only to a narrow range of frequencies for intensities near threshold. More intense tones resulted in neural responses to a broader range of frequencies. Most recordings were obtained from the more responsive middle cortical layers. However, radial penetrations yielded similar best frequency responses throughout the cortical layers. Occasionally, recording conditions were not optimal, and neurons at some locations within A-I responded weakly or not at all to auditory stimuli.

Both the tonotopic organization and isofrequency contours were revealed by relating best frequencies of neurons to the locations of electrode penetrations. Best frequencies ranged from less than 5 kHz to 30 kHz. Neurons responsive to high frequencies were found caudomedially, whereas neurons activated by low frequencies were located rostralaterally in A-I. Thus in both cases 87-22 (Fig. 3) and 87-45 (see Fig. 8), progressions from high to low best frequencies were found in the caudomedial to rostralateral direction, and results from other cases were similar. Electrode penetrations that extended into the ventral (or lateral) bank of the lateral sulcus (e.g., see Fig. 8) revealed that neurons with similar best frequencies were aligned in approximately a caudolateral to rostromedial direction. Similar orientations for isofrequency contours were seen in two other cases. Although mapping was less complete for tamarin 87-22 (Fig. 3), the isofrequency lines also appear to be oriented in a caudolateral to rostromedial direction.

The borders of A-I were estimated by changes in neural responsiveness. When electrode penetrations encountered neurons with reduced responsiveness to auditory stimuli (see below), these penetrations were judged to be on or near a physiological border of A-I. These penetrations were



Tamarin 87-22



Tamarin 87-44

○ Rhodamine injection sites
 □ Fast Blue injection sites
 ● HRP-WGA injection sites
 2.0 mm

Fig. 2. The locations of injection sites in A-I for two tamarins. Cortex has been removed from the rest of the brain, unfolded and flattened. Each animal received injections of three tracers within physiologically and architectonically defined A-I. Solid lines mark distinct myeloarchi-

tectonic borders, dashed lines mark less distinct borders, DL, dorso-lateral area. Other abbreviations as in Figure 1. Compare with Figure 1 for orientation. Connection patterns are shown in Figures 5 and 6.

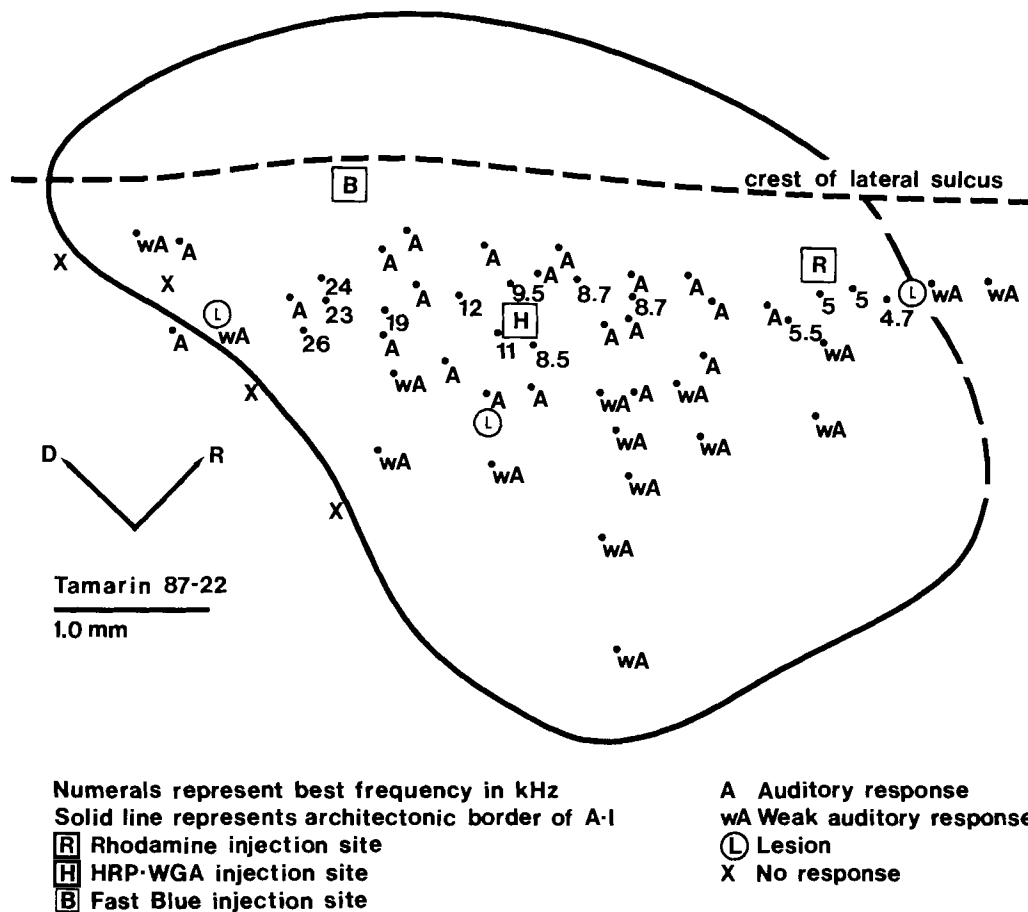


Fig. 3. Distribution of best frequencies for recording sites in the primary auditory area (A-I) of the right hemisphere for tamarin 87-22. Note the progression of high to low frequencies in a caudodorsal (or caudomedial) to rostroventral (or rostrolateral) direction. The solid line represents the myeloarchitectonic border. D, dorsal; R, rostral.

sometimes marked with electrolytic lesions. Lesions judged to be at the rostral and caudal borders of A-I are indicated for tamarin 87-22 in Figure 3. Lesions were also placed in locations of interest within the borders of A-I.

Neurons in cortex surrounding A-I usually did not respond well to pure tones; consequently best frequencies were not determined. However, responses to auditory stimuli were sometimes obtained. Of seven penetrations judged to be within the architectonically defined rostral area (R, located rostral or rostrolateral to A-I), three exhibited strong, nonhabituating neural responses to click stimuli, two showed weak responses (Fig. 3), and two yielded no response to auditory stimuli. Cortex immediately caudal to A-I was largely unresponsive to auditory stimulation. Neurons in 10 penetrations in this region were unresponsive to clicks or tones; three sites were responsive to auditory stimuli (Figs. 3 and 8; others not shown). In cortex caudomedial to A-I, five penetrations in a single animal yielded robust, nonhabituating responses to click stimuli. Cortex medial to A-I was weakly responsive (two penetrations) or not responsive (four penetrations) to click stimuli. No responses to auditory stimulation were recorded immediately lateral to A-I (four penetrations). Thus under our recording condi-

tions, cortex rostral or rostrolateral and caudomedial to A-I were moderately responsive to auditory stimuli, whereas the other cortical regions surrounding A-I were either weakly responsive or unresponsive.

Myeloarchitecture of A-I and surrounding regions. Each cerebral hemisphere was manually flattened and cut parallel to the surface and a series of sections was stained for myelin. Since some curvature of the cerebral cortex remained after the flattening process, single sections did not always reveal the total extents of various cortical fields. Thus different densities of myelin in a single flattened section reflect both areal variations and laminar differences as different cortical depths appear across the section. However, by examining and superimposing sections from several depths, borders could be consistently and reliably determined with good agreement across observers.

The general locations of architectonically defined subdivisions of cortex in flattened preparations are shown for two tamarins in Figure 2. Visual area 17 (or V-I) in the occipital cortex is always easily distinguished from adjoining area 18 (or V-II). A very densely myelinated middle temporal visual area (Allman and Kaas, '71) is readily seen (also see Fig. 4), whereas the dorsolateral visual field (Allman and Kaas, '74)

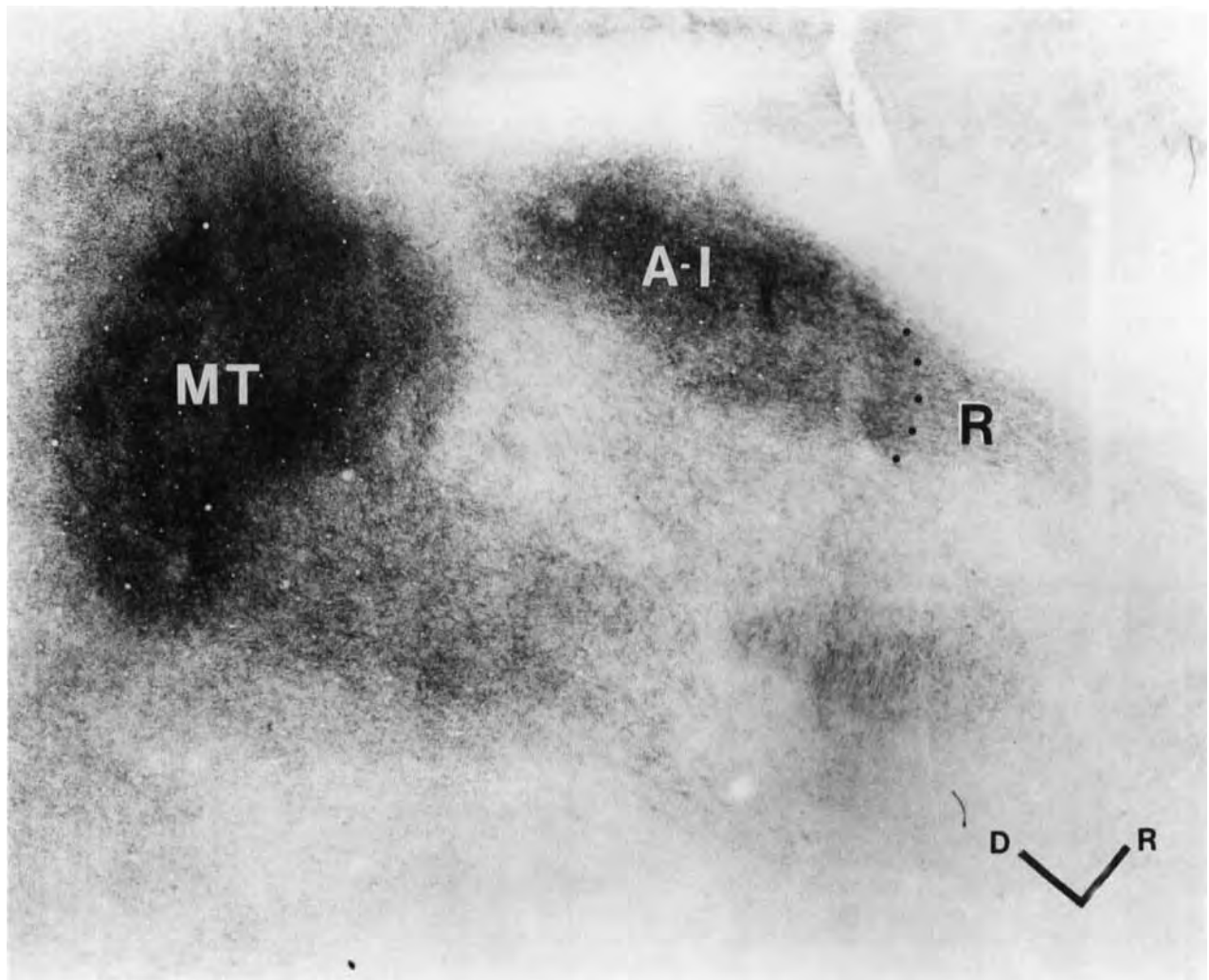


Fig. 4. Lightfield photomicrograph of the myeloarchitecture of a portion of unfolded, flattened temporal cortex. Note intense staining of A-I and the middle temporal area (MT). Direction bars = 1 mm. Other abbreviations as in previous figures.

is less densely myelinated. In the parietal cortex, primary somatosensory cortex (area 3b) is usually evident as a densely myelinated region (Krubitzer and Kaas, '86). The second somatosensory field, S-II, usually could be distinguished as a zone of moderate myelination (see Krubitzer and Kaas, '86). Other somatosensory fields were apparent, but were not included in the drawings.

In the middle and deep layers of cortex of the temporal lobe, A-I appears as a darkly stained oval, approximately 4–5 mm long and about 2–3 mm wide (Fig. 4). In superficial sections, A-I is lightly to moderately myelinated. Rostral to A-I, we distinguish a field that may correspond to the rostral area, R, of owl monkeys (Imig et al., '77). This rostral or rostralateral auditory region (R) is very lightly myelinated in superficial cortical sections and more moderately myelinated in deeper sections. The borders of R are not as clear as are those of A-I. Cortex surrounding A-I and R is less densely myelinated. Minor regional differences exist, but myeloarchitectonic subdivisions related to previously pro-

posed fields (e.g., the caudomedial, posterolateral, and anterolateral fields of the owl monkey; Imig et al., '77) were not obvious.

In the cytochrome oxidase preparations, V-I was obvious, and a banding pattern was observed in V-II. Areas MT, 3b, and A-I reacted somewhat more densely than surrounding cortex. However, the sections stained for myelin more clearly denoted these fields, including A-I.

Cortical connections

Intrinsic connections. The intrinsic connections of A-I appear to be preferentially distributed along isofrequency contours and, to a lesser extent, across isofrequency contours. Different aspects of intrinsic connectivity of A-I were revealed by small and large injection sites. Rhodamine and diamidino yellow injections invariably produced the smallest injection sites. The pattern of intrinsic label resulting from these small injections was similar for placements in low (Fig. 5; also tamarin 87-29, not shown), middle

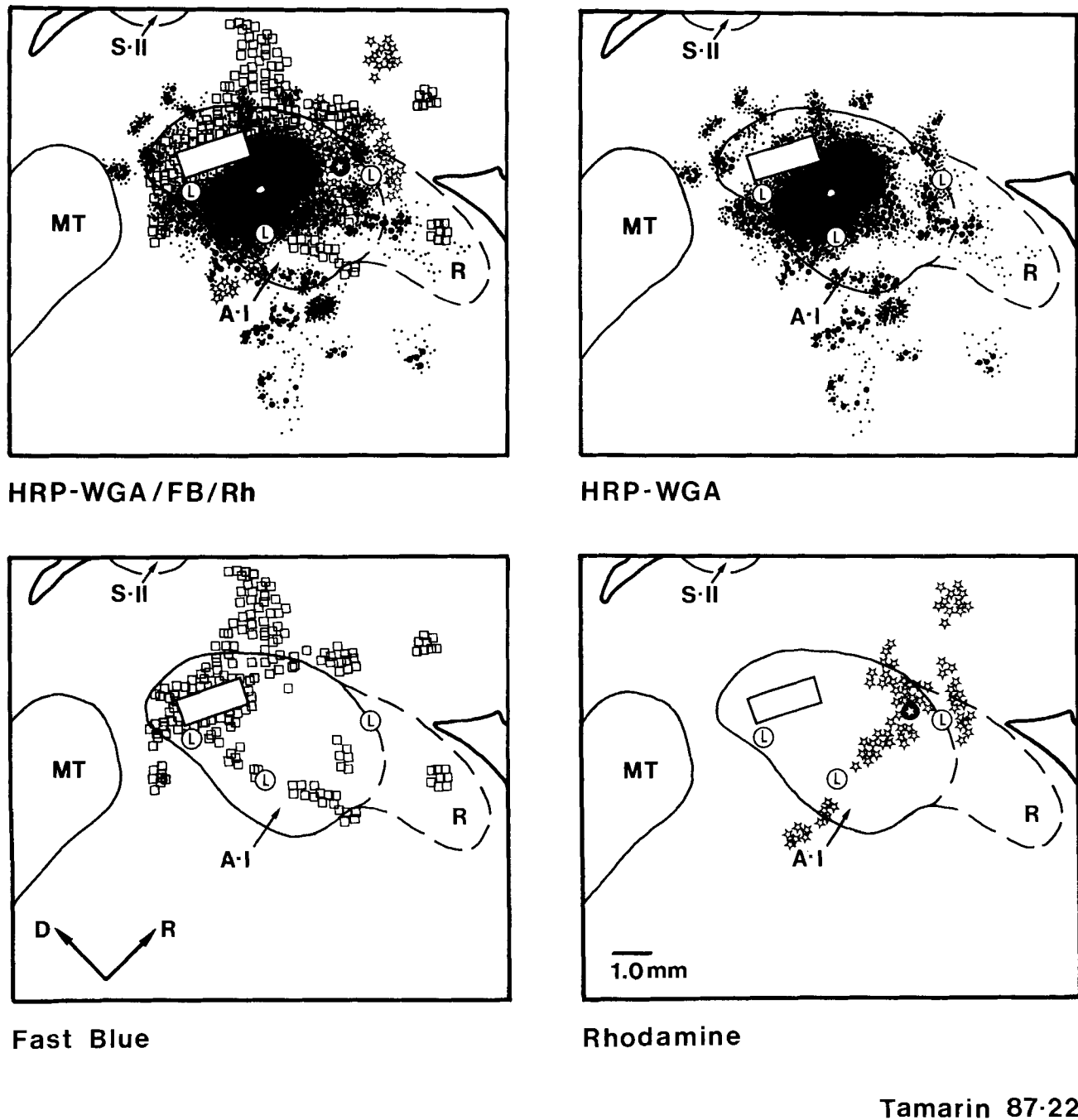


Fig. 5. Ipsilateral cortical connections of A-I for tamarin 87-22. Top left panel shows distribution of injection sites and transported label for all three tracers. Other panels show injection site and distribution of transported label for each tracer (as indicated). The large box indicates the rectangular necrotic zone produced by injection of fast blue. This zone probably includes the zone of effective uptake (see Methods). Anterogradely and retrogradely transported HRP-WGA drawn as small

and large dots, respectively; retrogradely transported fast blue, boxes; retrogradely transported rhodamine, stars. The circled star, the injection site for rhodamine. Label was drawn from several brain sections and superimposed to form a composite illustration. The tonotopic organization of A-I for this case is shown in Figure 3. Injections were placed in cortex best activated by 5kHz, (rhodamine), 10kHz (HRP-WGA), and about 25 kHz (fast blue). Abbreviations same as in previous figures.

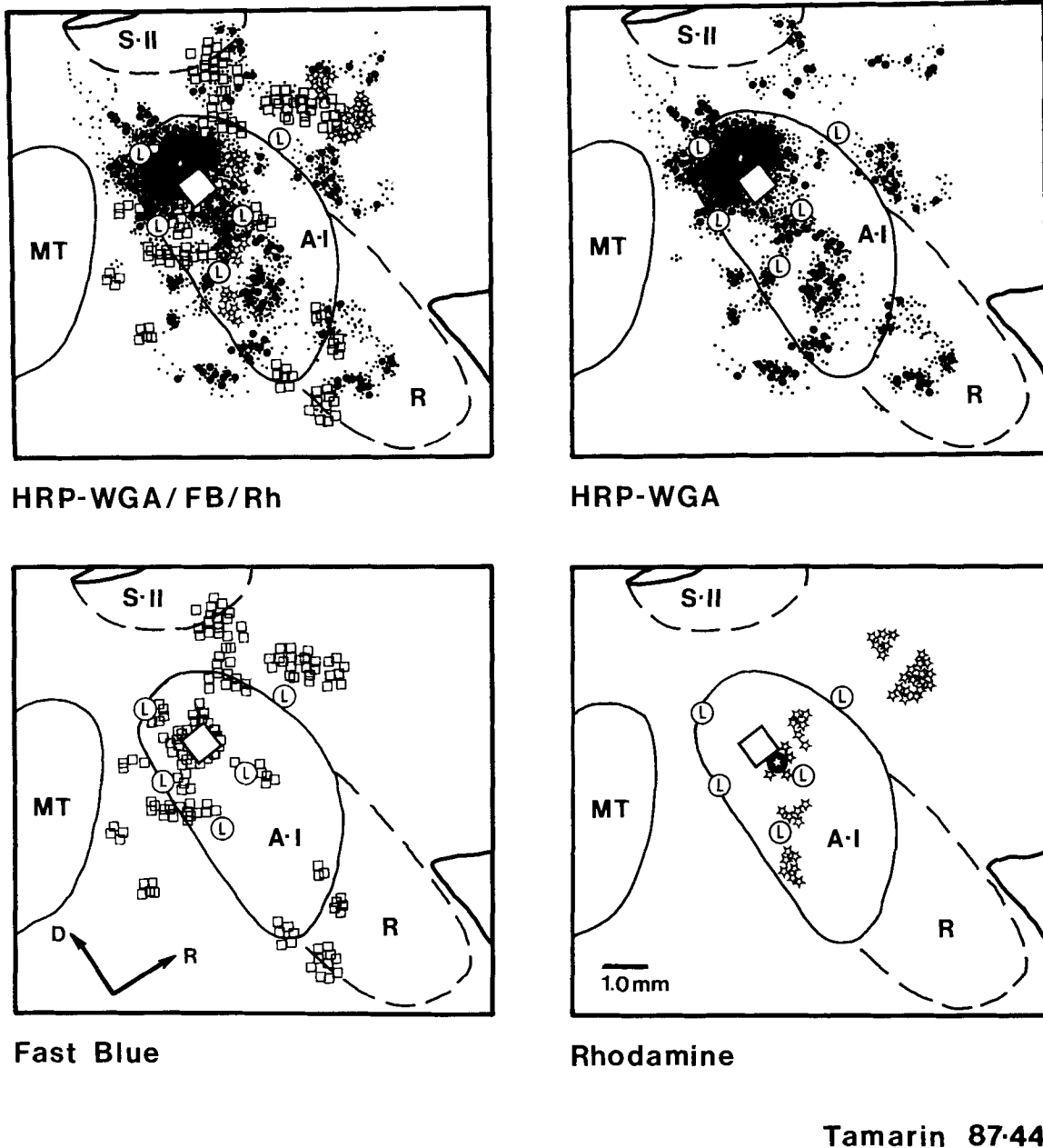
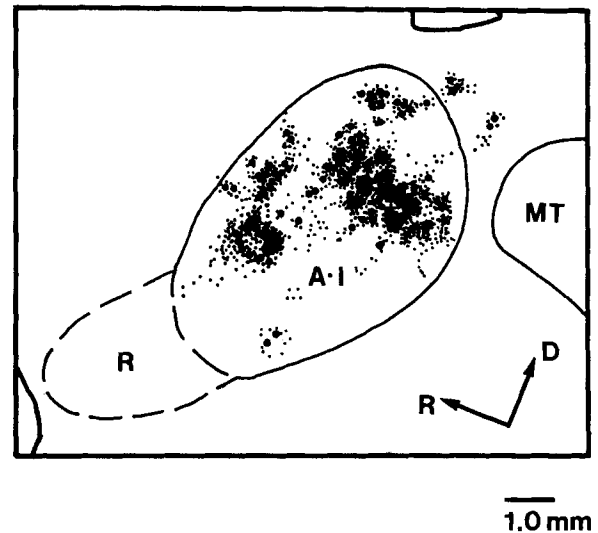
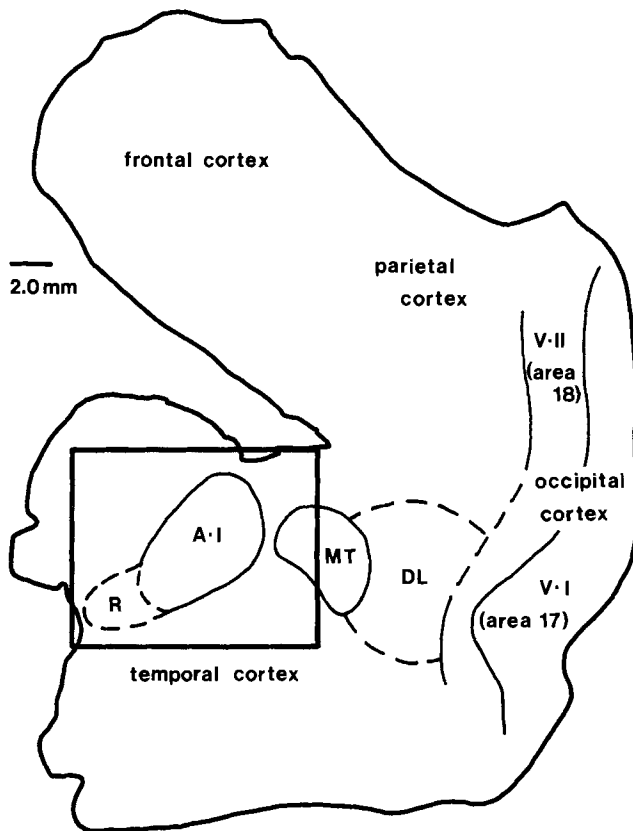


Fig. 6. Ipsilateral cortical connections of A-I for tamarin 87-44. Conventions as in Figure 5.

(Fig. 6) or high frequency regions (injection site shown in Fig. 8). In all cases, the injections produced a band of labeled cells oriented roughly in a rostromedial to caudolateral direction (e.g., Figs. 5, 6). The orientation of these bands of label approximately paralleled the presumed or demonstrated isofrequency contours in each case (e.g., compare Figs. 3 and 5). Thus neurons in frequency domains across A-I appear to have interconnections oriented along the isofrequency contours.

Evidence for more widespread intrinsic connections was provided by the larger injections. The intrinsic label following injections of fast blue into A-I was not as restricted as that seen with rhodamine or diamidino yellow. Although the majority of the labeled cells resulting from a fast blue injection formed a band of label usually extending rostromedially to caudolaterally from the injection site (i.e., along isofrequency contours), additional foci of label within A-I were quite distant from the injection site (Figs. 5, 6). The



Tamarin 87-22

Fig. 7. Contralateral cortical connections of A-I for tamarin 87-22. Left panel is the unfolded, flattened hemisphere contralateral to HRP-WGA injection in A-I. The boxed region is magnified at right and shows

the distribution of transported label in A-I and in cortex just caudomedial to A-I. Note dense, reciprocal, and patchy connections with the central portion of A-I.

intrinsic connections demonstrated following HRP-WGA injections were even more widespread than those seen following injections of fast blue. The HRP-WGA injection sites were relatively large. Nevertheless, the label immediately adjoining the injection sites appeared to extend preferentially along the isofrequency contour (e.g., Fig. 8). In addition, small patches of label were scattered throughout A-I following HRP-WGA injections (Figs. 5, 6, 8). These scattered foci were more numerous than those present following fast blue injections. Within A-I, anterogradely and retrogradely transported HRP-WGA usually occurred together.

In summary, the most prominent intrinsic ipsilateral connections of A-I were oriented along the isofrequency contours. Larger injection sites revealed other scattered foci of intrinsic connections in regions of A-I with neurons of different best frequencies.

Ipsilateral connections. The results indicate that A-I is interconnected with a belt of cortex immediately surrounding A-I. Single locations in A-I, regardless of frequency, project to multiple sites in this belt (Figs. 5, 6, 8). In addition, foci of label were found in more distant regions of cortex in some cases. However, the different tracers varied in the number of cortical sites that they labeled (e.g., Fig. 5), indicating differences in the effectiveness of the tracers

under the conditions of the experiment. Typically more foci of label were seen following HRP-WGA than fluorescent tracer injections (e.g., compare Figs. 5, 6, 8).

The results provide evidence that A-I is topographically connected with at least two, and possibly three, adjoining cortical regions. The topographic patterns were best demonstrated in cases with injections of three different tracers. For example, in tamarin 87-22 (Fig. 5), rhodamine and HRP-WGA were centered in regions that had best frequencies of approximately 5 kHz and 10 kHz, respectively, whereas fast blue was placed in a region presumed to have higher best frequencies (see Fig. 3). The resulting pattern of transported label within the rostral area (R, defined on the basis of myeloarchitecture as described above) was topographically organized. The upper left panel of Figure 5 shows a near "mirror-image" reversal of the pattern of transported label in R when compared to the pattern of the injection sites in A-I. Thus when rhodamine was placed close to the A-I/R border within A-I, this rhodamine was transported to neurons close to the A-I/R border within R. Fast blue, placed far from the A-I/R border within A-I, was transported to cells far from the A-I/R border within R. Finally, HRP-WGA, placed between fast blue and rhodamine within A-I, was transported to an intermediate region within R.

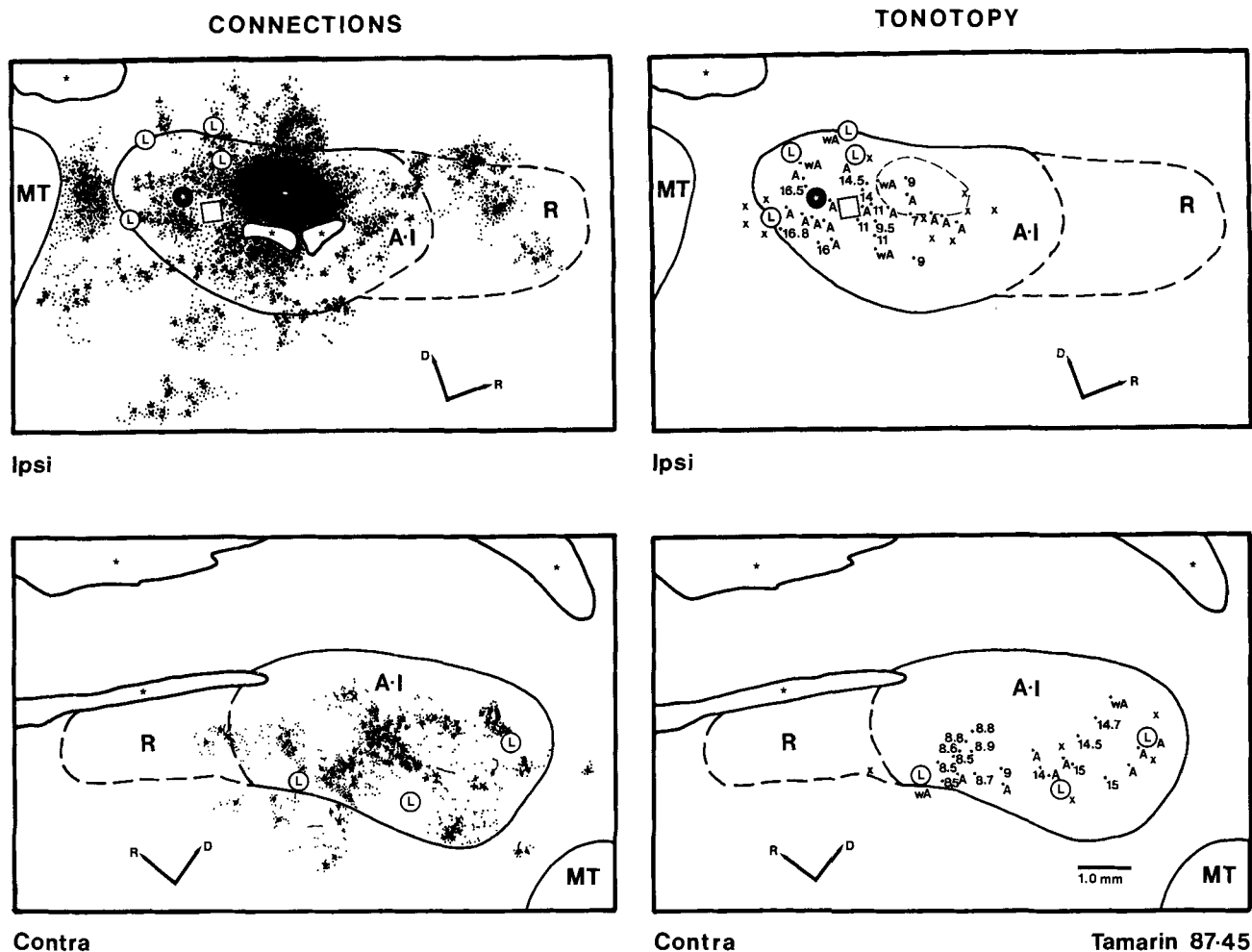


Fig. 8. Cortical connections and response characteristics of multi-unit recording sites for A-I of both hemispheres in tamarin 87-45. Upper left panel shows the locations and extents of injections of rhodamine (circled star), fast blue (square) and HRP-WGA (black oval) into A-I, as well as the transported HRP-WGA. Upper right panel shows the locations and extents of the injection sites with respect to the tonotopic organization of A-I. Injections involved cortex representing approxi-

mately 9kHz (HRP-WGA), 14 kHz (fast blue), and 16 kHz (rhodamine). Lower left panel illustrates the contralateral cortical connections resulting from the transport of HRP-WGA. The tonotopic organization of the contralateral A-I is seen in the lower right panel. Asterisks indicate tears in the tissue. Other conventions and abbreviations as in previous figures.

Cortex caudolateral to A-I also appears to have topographically organized connections with A-I. The upper left panel of Figure 5 shows that the pattern of labeled cells caudolateral to A-I parallels that of the injection sites. That is, the lateral to medial progression of injection sites of fast blue, HRP-WGA, and rhodamine produced a lateral to medial progression of cells labeled with fast blue, HRP-WGA, and rhodamine in the region caudolateral to A-I. Although rhodamine and diamidino yellow failed to label this region in all other cases (e.g., Fig. 6), there was a similar pattern of topography where transported label paralleled the injection sites for the fast blue and HRP-WGA in two other cases. The partial overlap of the HRP-WGA and fast blue injec-

tion sites in case 87-44 (Fig. 6) resulted in more overlap in the transported label, so the pattern was less clear.

Dense foci of label were consistently found in the region medial to A-I (Figs. 5, 6). Whereas the pattern of topography was not completely clear, a "parallel" tonotopic pattern was suggested by the connections (e.g. Figs. 5, 6). Other connections were with cortex rostromedial to A-I and lateral to A-I (seen via HRP-WGA injections in Figs. 5, 6, 8). It is not certain if these are additional fields or parts of the medial and caudolateral regions described above.

In summary, A-I appears to be surrounded by auditory cortex. Patterns of transported label indicate that A-I is topographically connected with fields located rostral, cau-

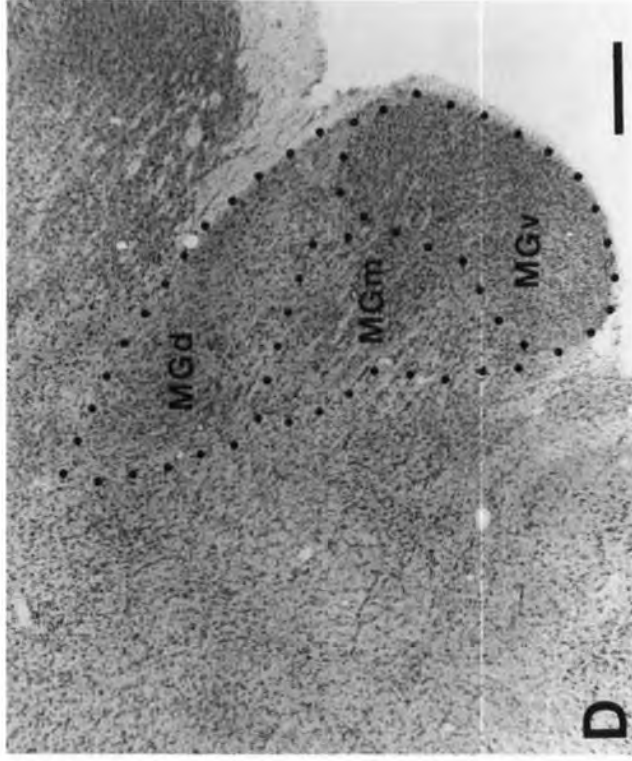
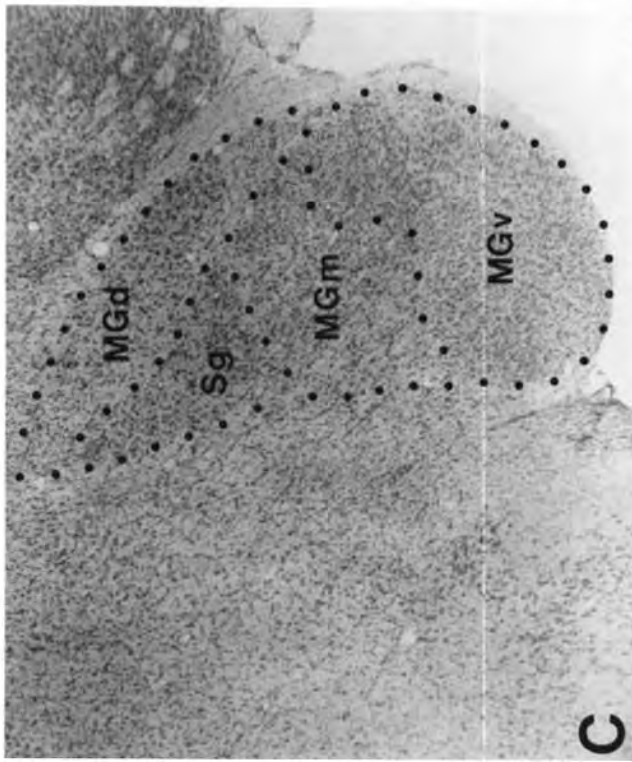
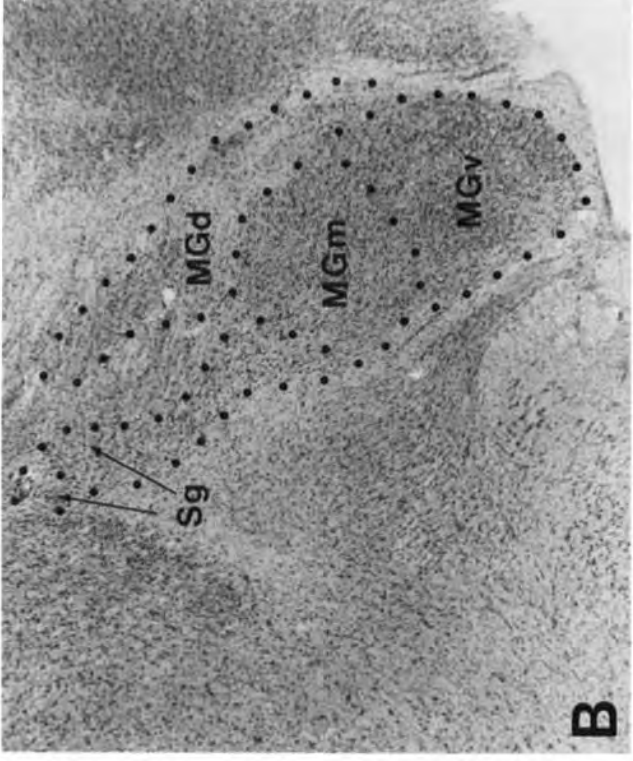
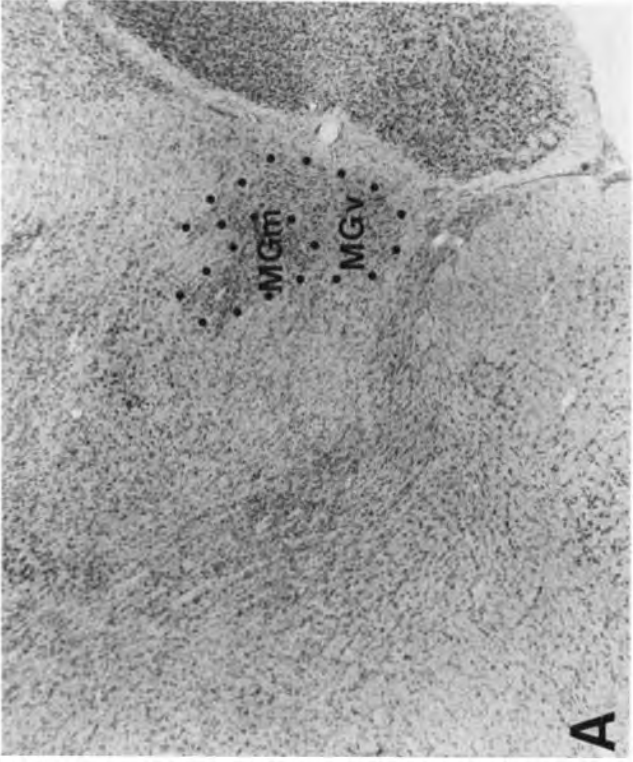


Figure 9

dolateral, and possibly medial to A-I; A-I is also interconnected with other regions of cortex located rostromedial and lateral to A-I.

Contralateral connections. The patterns of callosal connections were determined from the HRP-WGA injections. In all HRP-WGA cases, labeled terminals and cells were found in the contralateral cortex, and label was noted in the corpus callosum. In no case were fluorescently labeled callosally projecting cells observed, probably as a result of the relatively short postinjection survival times (see Methods).

The callosal connections of A-I were almost solely with A-I of the opposite hemisphere. In addition, the major callosal connections were topographically matched. Thus in all cases, foci of label were found mainly in A-I, and the densest focus of label appeared to be in a position in A-I comparable to that which received the injection (e.g., Figs. 7, 8). For example, in cases in which the middle portion of A-I received the injection (Fig. 2, left panel, and Fig. 8, upper left panel), the densest focus of label was found in the middle portion of the contralateral A-I (Fig. 7, right panel, and Fig. 8, lower left panel). The topography of these contralateral connections was also apparent when higher frequency or more caudomedial regions of A-I (Fig. 2, right panel) or lower frequency or more rostralateral regions of A-I received the injections of HRP-WGA. Furthermore, these foci of label formed bands that were oriented in a rostromedial to caudolateral (Fig. 7) or in a medial to lateral (Fig. 8) direction, similar to the pattern seen for the ipsilateral intrinsic label.

In order to examine the topography of the contralateral connections more closely, A-I of both the ipsilateral and the contralateral hemispheres of each of two tamarins were electrophysiologically defined and marker lesions were placed at physiologically defined locations. Later, patterns of connections were related to the physiological and myeloarchitectonic data. Figure 8 shows the results of one such case. In this tamarin, HRP-WGA was injected into a region with a neural best frequency of 9 kHz. The injection site spread to include cortex responsive to both lower (≤ 7 kHz) and higher (≥ 9 kHz) frequencies (see Fig. 8, upper panels). In the contralateral hemisphere, a dense focus of label was in a region of cortex most responsive to pure tones ranging from 8.5 kHz to ≤ 14 kHz (Fig. 8, lower panels). This frequency range is similar to the frequency range of the cortex that received the injection in the opposite A-I. Furthermore, the densest callosal label clustered to form a band oriented approximately parallel to the isofrequency contours (see lower right panels). Injections in A-I also produced additional, less dense zones of label that were found scattered throughout the contralateral A-I in both higher and lower frequency regions (Figs. 7, 8). A few labeled terminals and cells were found outside of A-I, but the location of this label was not consistent from case to case (e.g., compare Figs. 7 and 8). Similar results were obtained in another case where A-I contralateral to the injection was mapped.

In summary, the contralateral cortical connections of A-I were almost exclusively with A-I. Single restricted injections produced scattered foci of label in contralateral A-I, with the densest label clustered in a band oriented approximately parallel to the isofrequency contours. This dense label was in a best frequency region that matched that of the injection site.

Architectonic features of the auditory thalamus

The injections in A-I revealed connections with subdivisions of the auditory thalamus and with parts of the inferior colliculus. In the Nissl-stained brain sections from the experimental tamarins, it was possible to identify nuclei and other subdivisions of the brain stem that have been previously described in other primates and other mammals (Fig. 9). The major thalamic auditory region, the medial geniculate complex (MG), traditionally has been subdivided into a principal or ventral nucleus (MGv), a magnocellular or medial nucleus (MGm), and a dorsal nucleus (MGd) (see Jones, '85). Other thalamic subdivisions that have been related to the auditory system include the supragenulate nucleus (Sg), the caudal extension of the posterior complex (Po), and, occasionally, the limitans nucleus (Li).

Ventral division of the MG. The principal or ventral division of the MG (MGv) occupies a ventral or ventrolateral position and extends from the rostral pole to near the caudal pole of the complex. The MGv is distinguished by relatively small, tightly packed neurons (Fig. 9) and light staining for myelin. The MGv is surrounded by very densely staining myelinated fibers. The MGv reacts much more darkly for cytochrome oxidase than do surrounding structures.

Medial division of the MG. The MGm is dorsomedial to the MGv and extends throughout most of the complex. The MGm is populated by cells that range widely in size. Because many of the cells are large, the nucleus is commonly referred to as the magnocellular division of the complex. In general, neurons in the MGm are packed more loosely than those in the MGv but more tightly than those in the MGd. Cell-sparse striations running dorsomedial to ventrolateral are obvious in the MGm (e.g., Fig. 9D); these striations stain darkly for myelin and they presumably correspond to the incoming fibers of the brachium of the inferior colliculus. As a result of the densely stained fibers, the MGm is more densely myelinated than adjacent nuclei of the MG. The MGm reacts less darkly for cytochrome oxidase than the MGv or the MGd, and the myelinated fibers of the brachium of the inferior colliculus demonstrate little cytochrome oxidase activity.

Dorsal division of the MG. The dorsal division of the MG (MGd) forms a sliver or a "cap" on the dorsolateral aspect of the MG complex (Fig. 9). The MGd resembles the MGm in having a range of cell sizes and densely stained cells, but MGd has a lower packing density of neurons (Fig. 9). Similar to the MGv, the MGd stains very lightly for myelin and is surrounded by densely stained fibers. In tissue reacted for cytochrome oxidase, MGd is more lightly stained than the MGv and slightly more darkly stained than the adjacent MGm, Sg nucleus, and more dorsal structures.

Supragenulate nucleus. The supragenulate nucleus (Sg) is located dorsomedial to the MGm and extends throughout the rostral two-thirds of the MG complex. Darkly staining and relatively medium- to large-sized cells characterize the Sg and distinguish the Sg from surrounding

Fig. 9. Lightfield photomicrographs of Nissl-stained frontal sections through the medial geniculate complex of a tamarin in a rostrocaudal sequence. Proposed subdivisions are outlined with dots. MGd, MGm, MGv, dorsal, medial, and ventral divisions of the medial geniculate complex, respectively; Sg, supragenulate nucleus. Approximate stereotaxic A-P levels: A, A4.5; B, A4; C, A3.5; D, A3. Scale bar = 0.5 mm. Lateral is right.

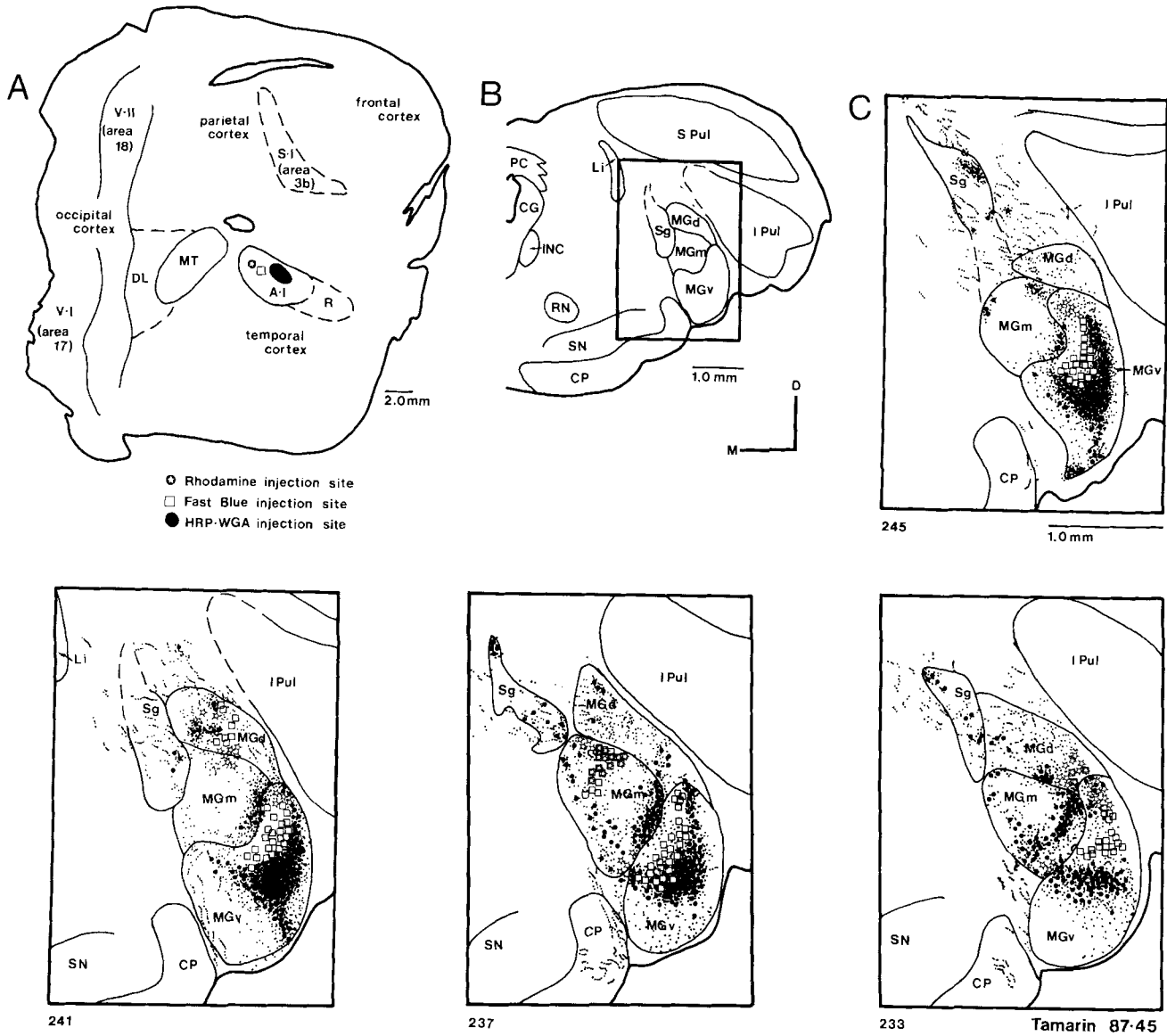


Fig. 10. Thalamic connections of A-I for tamarin 87-45. A. Unfolded, flattened cortical hemisphere showing the locations and extents of injection sites of three tracers (HRP-WGA, fast blue, and rhodamine) in A-I (as defined by physiology and myeloarchitecture). B. Frontal section 241 of the thalamus showing the medial geniculate complex with respect to surrounding structures. C. Thalamic label from injections of three tracers (each in a different frequency representation in A-I) indicated in panel A, in a rostral (#245) to caudal (#233) frontal series of

40- μ m brain sections. Injections involved cortex representing approximately 9kHz (HRP-WGA), 14 kHz (fast blue), and 16 kHz (rhodamine). Dense topographic connections are seen with the MGv, whereas less label is seen in the MGm and MGd. Sparse label is found in the Sg nucleus. CG, central gray; CP, cerebral peduncle; INC, interstitial nucleus of Cajal; I Pul, inferior pulvinar; Li, nucleus limitans; PC, posterior commissure; RN, red nucleus; S Pul, superior pulvinar. Other abbreviations and conventions as in previous figures.

nuclei (Fig. 9). Myeloarchitecturally, the Sg appears very similar to the MGm, with the darkly staining fibers from the brachium of the inferior colliculus coursing through this nucleus. In cytochrome oxidase material, the Sg resembles the MGm, but the Sg is distinguished from the more darkly stained medial and dorsal tissue.

Thalamic connections

Ventral division of the MG. All injections labeled cells or cells and fibers in the MGv. Because the tracers were

placed in different frequency representations in A-I, the patterns of transported tracers revealed the topography of connections with MGv. For example, in tamarin 87-45 (Fig. 10), rhodamine, fast blue, and HRP-WGA were placed in regions with neural best frequencies of approximately 16 kHz, 14 kHz, and 9 kHz, respectively (see Fig. 8). Although the HRP-WGA injection site spread to both higher and lower frequency regions, none of the injection sites overlapped (Fig. 10A). As a result of the injections, rhodamine labeled cells were found in the dorsal region of the MGv,



Fig. 11. Darkfield photomicrograph of transported HRP-WGA in the MGv, MGm, MGd, and Sg in section #241 (drawn in Fig. 12C) of tamarin 87-45 resulting from injection of HRP-WGA confined to A-I. Injection site placed in a middle frequency region of A-I as shown in Figure 8. Scale bar = 0.5 mm. Frontal section; medial is left.

HRP-WGA labeled cells and terminals were located in a more ventral portion, and fast blue labeled cells occupied an intermediate position (Fig. 10C). This pattern of label suggests a dorsal to ventral progression of high to low frequency representation in the MGv.

In case 87-45, the transported HRP-WGA formed a crescent-shaped zone of label throughout all but the caudal pole of the MGv (Fig. 10C; also see Fig. 11). Although most of this crescent of label occupied a region ventral to the zone of fast blue labeled cells, a portion of the crescent extended into a more dorsolateral part of the MGv, and there was some overlap of the fast blue and HRP-WGA labeled cells in the MGv (Fig. 10C, section 237). This overlap was not due to an overlap of injection sites; rather, the HRP-WGA injection site spread into regions of A-I containing neurons responsive to frequencies up to 11 kHz. This frequency was also the

best frequency of neurons that received the fast blue injection (see Fig. 8). Thus the overlap of transported HRP-WGA and fast blue in the MGv appears to be due to the separate injection sites encroaching upon different regions of the same isofrequency contour. However, no double-labeled neurons were observed in the MGv.

Tamarins 87-22 and 87-29 also provided evidence for a tonotopic organization in the MGv. In tamarin 87-22 (Fig. 12), rhodamine and HRP-WGA were placed in cortex that had best frequencies of approximately 5 kHz and 10 kHz, respectively, whereas fast blue was injected into a higher frequency region of about 25 kHz (see Fig. 3). As in other cases, the HRP-WGA injection site spread to include both higher and lower frequency regions (Fig. 2, left panel). As a result of these injections, rhodamine label was in more ventral, fast blue in more dorsal, and HRP-WGA was in inter-

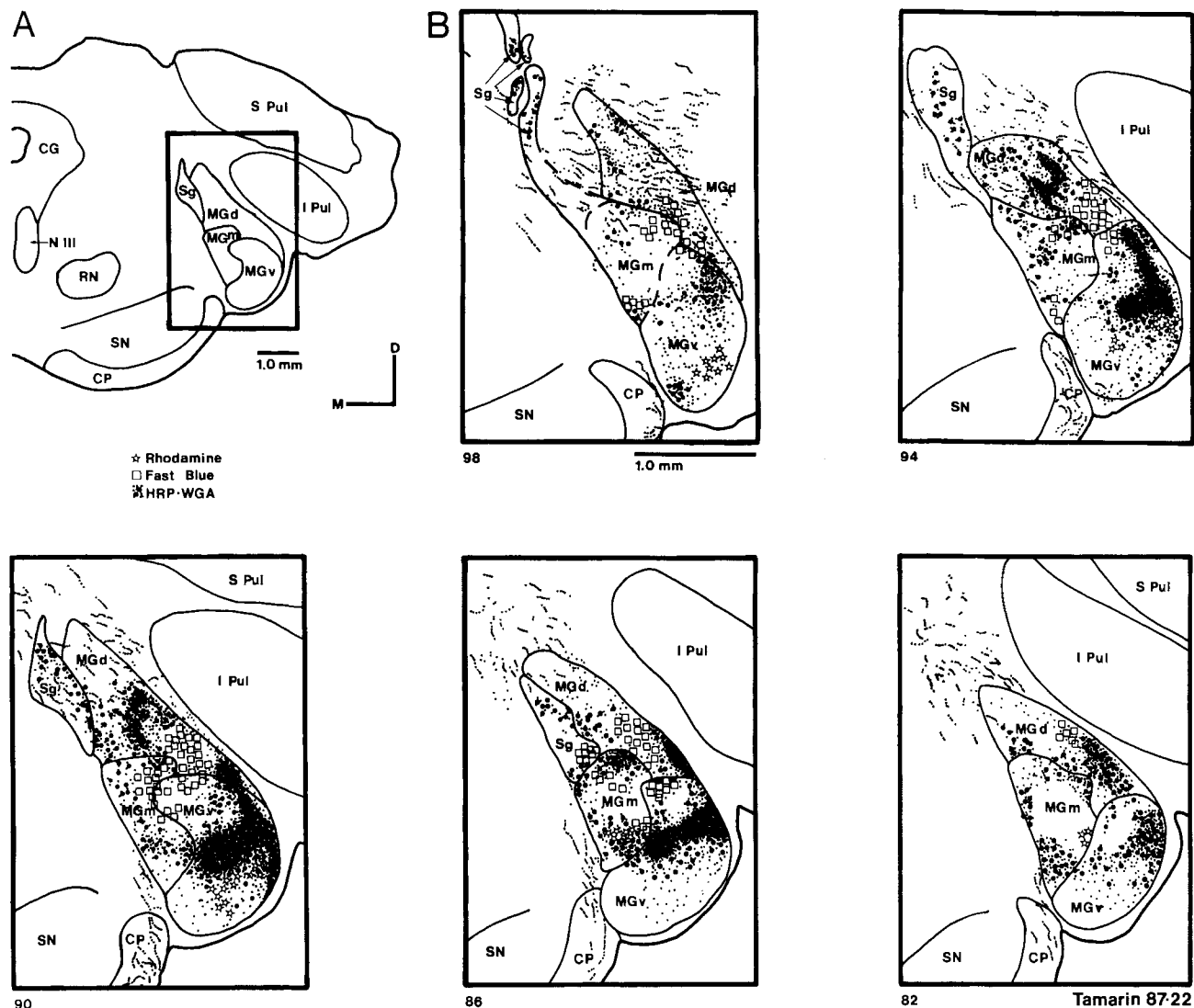


Fig. 12. Thalamic connections of A-I for tamarin 87-22. **A.** Frontal section of the thalamus showing the MG complex with respect to surrounding structures. **B.** Thalamic label resulting from injections of three tracers, each in a different frequency representation in A-I (shown in Fig. 2), in a rostral (#98) to caudal (#82) series of 40- μ m frontal sections.

mediate regions of the MGv. Supportive, though less compelling evidence for a dorsal to ventral representation of high to low frequencies in the MGv was obtained in three other cases. In tamarin 87-29, fast blue, HRP-WGA, and diamidino yellow were centered in regions of A-I with best frequencies of approximately 17 kHz, 11.5 kHz, and 9 kHz, respectively. The HRP-WGA injection site, however, spread to largely overlap with the fast blue injection site. Although the expected pattern of labeled neurons was seen in the MGv (diamidino yellow, ventral; fast blue, dorsal; HRP-WGA, interposed), there was extensive overlap of the HRP-WGA and fast blue label. Injections of HRP-WGA, fast blue, and rhodamine were placed in relatively high, middle, and low frequency regions, respectively, within A-I for

tamarin 87-22. Injections involved cortex representing approximately 5kHz, (rhodamine), 10 kHz (HRP-WGA), and about 25 kHz, (fast blue). Note dense, topographic connections with the MGv, and less dense connections with the MGm, MGd, and Sg. Other abbreviations and conventions as in Figure 10.

tamarin 87-44 (Fig. 2). Although neurons labeled with rhodamine were not observed in any portion of the thalamus in this case, cells labeled with fast blue cells and terminals labeled with HRP-WGA were found within the MGv. The HRP-WGA label was largely located dorsal to the fast blue label, although there was some overlap. The remaining

Fig. 13. **A.** Darkfield photomicrograph of section #90 in tamarin 87-22 (see Fig. 14) showing transported HRP-WGA in the MGd, MGm, MGv, and Sg nuclei. **B.** Lightfield photomicrograph of an adjacent section stained for Nissl substance, showing the subdivisions of the medial geniculate complex and the Sg nucleus. Arrows mark corresponding points on tissue sections. Other conventions and abbreviations as in previous figures. Scale bar = 0.5 mm. Frontal section; medial is left.

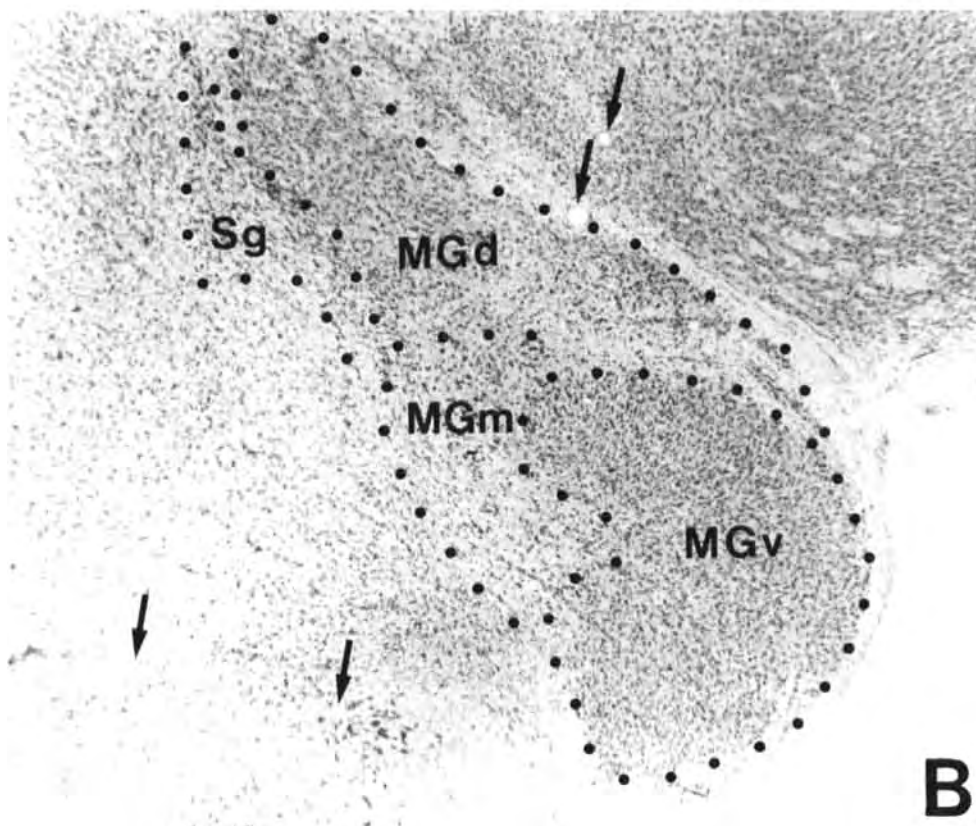


Figure 13

tamarin (87-60) received only an injection of HRP-WGA. The injection was placed into cortex in A-I where neurons had a best frequency of approximately 18 kHz, a relatively high frequency. As expected on the basis of data from other cases, dorsal portions of the MGv were labeled.

The ventralmost portion of the MGv was not labeled or only lightly labeled (e.g., Figs. 10, 12) across cases. Presumably, this is the lowest frequency region of the MGv and the relative lack of label in this region was probably due to the lack of injections in regions of A-I with neurons responsive to frequencies lower than 5 kHz.

The HRP-WGA injections also produced evidence that isofrequency contours course largely in a mediolateral direction in the MGv. The band of label produced by the HRP-WGA in tamarin 87-22 was oriented in a lateral to medial direction, with a slight lateroventral slant (Figs. 12B, 13A). This label extended from the lateral border of the MGv to its medial border. In addition, label spread dorsoventrally in the lateral part of the main column of label so that extensions of label perpendicular to the main column were observed. These results are consistent with the overall evidence that frequencies are represented from high to low in roughly a dorsoventral direction, whereas isofrequency contours course in roughly a mediolateral direction in the MGv. Although the HRP-WGA injection site was centered in a region responsive to approximately 10 kHz, the injection spread to include both lower (≤ 8.7 kHz) and higher (≥ 19 kHz) frequency regions (e.g., Figs. 2, 3). Thus, the resulting label would be expected to span part of the dorsoventral extent of the MGv. Furthermore, the injection site nearly extended to the rostromedial and caudolateral borders of A-I, thereby involving most of the 10 kHz isofrequency contour (again, compare Figs. 2 and 3). Thus the label resulting from an injection site spanning isofrequency contours would be expected to extend in a band oriented perpendicular to the high to low frequency progression. Similar labeling of presumed isofrequency contours in the MGv was seen in two other cases (87-29 and 87-44, not shown; however, see Fig. 2 for the location and extent of the HRP-WGA injection site for tamarin 87-44). As was seen for case 87-45 (Fig. 10), some overlap of fast blue and HRP-WGA was present in the MGv for tamarin 87-22 (Fig. 12). This was expected because the injection sites overlapped slightly (Fig. 2).

Medial division of the MG. Injections in A-I also labeled neurons or fibers and neurons in the MGm. The HRP-WGA label was more dense and widespread in the MGm than was the fast blue or rhodamine, and the amount of transported label was proportional to the size of the injection site. In general, the zones of labeled cells from the different tracers overlapped somewhat (e.g., Figs. 10, 12), even when the injection sites were completely separate (e.g., tamarin 87-45, Fig. 10). Within the overlap zones of cells labeled by different tracers, some cells were double labeled. Whereas no attempt was made to systematically determine the proportion of double-labeled neurons, different frequency regions of A-I receive input from some of the same single cells within the MGm. Although label was present throughout the rostral to caudal extent of the MGm, the label was invariably densest in the most caudal two-thirds of this nucleus (e.g., Figs. 10, 12; others not shown).

Whereas label from injections in different frequency regions of A-I overlapped, the results provided evidence for a crude topography in connections. The general tendency was for injections in high frequency zones of A-I to label more dorsomedial parts of the MGm than injections in low frequency zones (e.g., Figs. 10, 12).

Dorsal division of the MG. Injections in A-I also labeled neurons and axons in the MGd. Label was found scattered throughout the MGd in tamarins 87-45 and 87-29 (Fig. 10; others not shown), but was concentrated in the ventral portion of the nucleus in tamarins 87-22, 87-44, and 87-60 (Fig. 12; others not shown). Label was present throughout the rostral to caudal extent of the MGd but, in general, was less dense at both its rostral and caudal poles (e.g., Figs. 10, 12). Occasionally, double-labeled cells were present in the MGd, but they were less common than in the MGm. As with the MGm, the results provided some evidence for a crude topography in connections with the MGd. In general, injections in high frequency regions of A-I labeled more ventrolateral parts of the MGd than injections in low frequency regions (e.g., Fig. 10).

Supragenulate nucleus. Injections of HRP-WGA in A-I always resulted in labeled cells and terminals in the supragenulate nucleus (Sg), whereas injections of the fluorescent tracers rarely labeled this nucleus (e.g., Figs. 10, 12). The label was widely scattered throughout the rostral to caudal extent of the Sg (Figs. 10, 12) and extended into the limitans nucleus in two cases (87-22, 87-29).

In summary, the MGv has orderly topographic connections with A-I. MGv neurons connected with the part of A-I representing higher best frequencies are located dorsal to neurons connected with the part of A-I representing lower best frequencies. Isofrequency contours in MGv appear to be oriented in a largely medial to lateral direction. Both the medial and dorsal divisions of the MG project to A-I, and there is evidence for crude topographic patterns of connections. Double-labeled neurons were sometimes observed in the MGm and, to a lesser extent, in the MGd. The supragenulate nucleus also has connections with A-I, but these connections appear to be rather sparse and diffuse.

The inferior colliculus

Architecture. The inferior colliculus (IC) has been subdivided on the basis of Golgi material into the dorsal cortex (DC), the central, medial, and lateral portions of the central nucleus (C, M, and L, respectively), and regions surrounding these nuclei (Morest and Oliver, '84). In Nissl-stained frontal sections from the experimental brains, the central nucleus has smaller and generally less densely packed neurons than DC. Subdivisions of the central nucleus were difficult to distinguish, and the borders indicated in illustrations are approximate. Subdivision L is characterized by relatively loosely packed, medium to large-size cells and by a relative lack of staining in myelin preparations. M has larger and more darkly staining neurons. The DC has myelinated fibers coursing in a largely dorsolateral to ventromedial direction and is distinct from dorsal, medial, and lateral structures by being darkly stained in tissue reacted for cytochrome oxidase.

Connections. The projections to the inferior colliculus (IC) from A-I were analyzed from a total of four tamarins with HRP-WGA injections. Fluorescent label was not observed in the IC. In all cases (e.g., Fig. 14; see also Fig. 16),

Fig. 14. Transported label in the inferior colliculus (IC) in a rostral (#165) to caudal (#153) series of coronal sections after an injection of HRP-WGA in A-I in tamarin 87-45 (injection site shown in Fig. 8). Labeled axon terminals are found in bands that are oriented dorsomedial to ventrolateral in the dorsal cortex (DC) of the IC. Label is extremely sparse in the central part (C) of the central nucleus of the IC. CG, central gray; CIC, commissure of the IC; L, M, lateral and medial parts, respectively, of the central nucleus of the IC.

Projections to the inferior colliculus from A-I

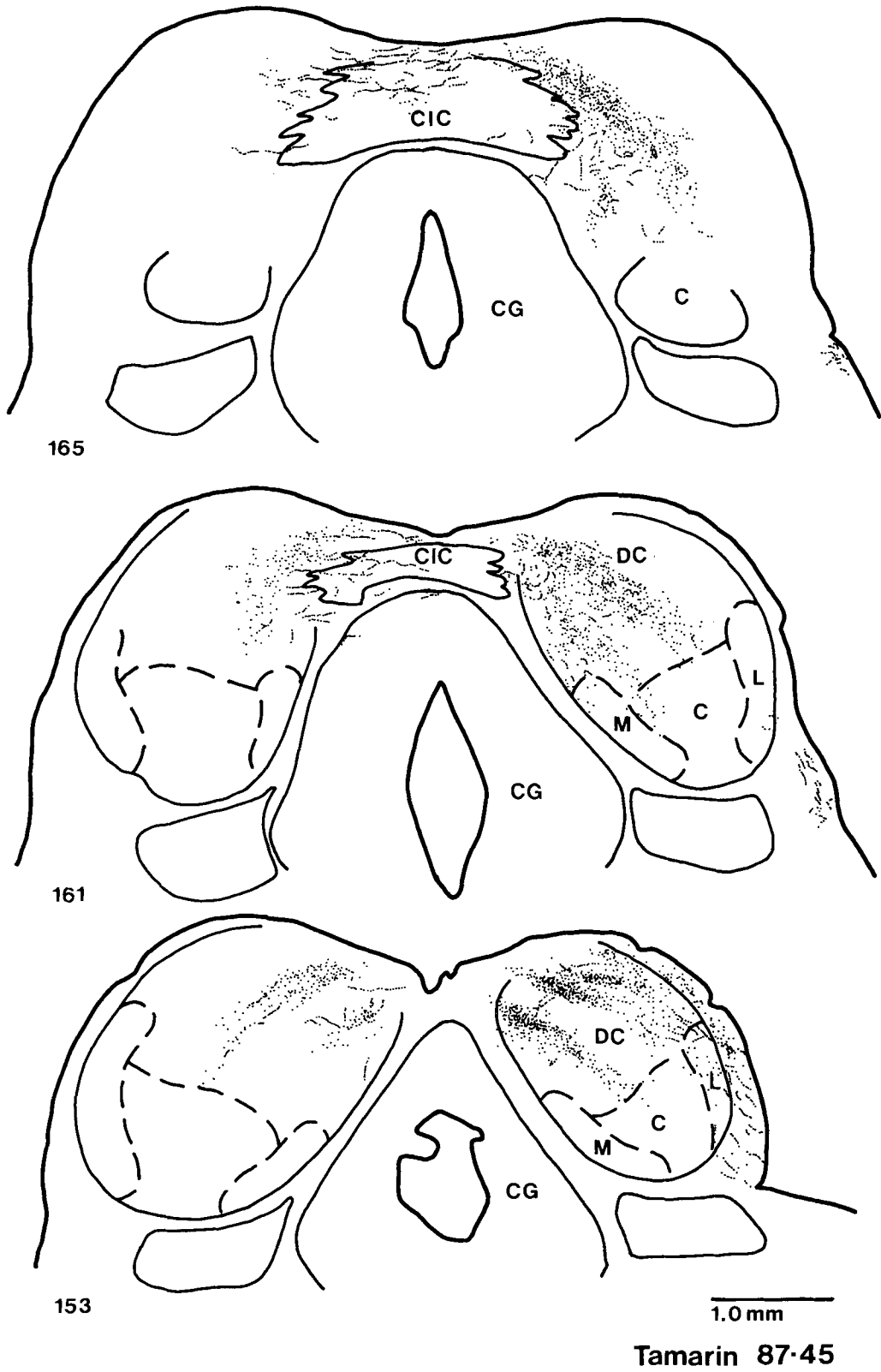


Figure 14

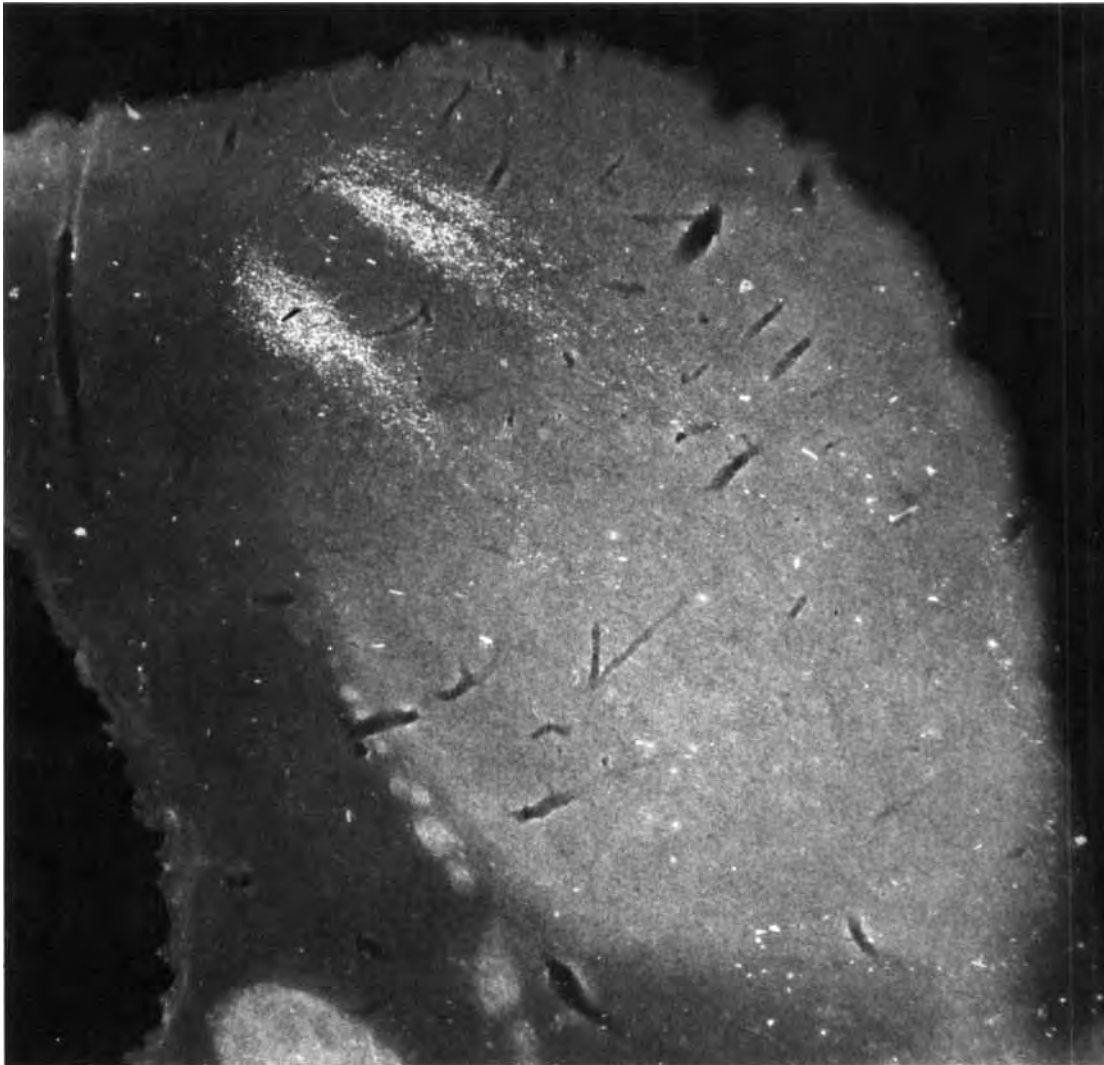


Fig. 15. Darkfield photomicrograph of section #157 showing labeled terminals in the DC of the IC in tamarin 87-45 (see Fig. 16) after an injection of HRP-WGA in A-I. Scale bar = 1.0 mm. Frontal section; medial is left.

labeled terminals were largely restricted to the dorsal cortex (DC) of the IC, with additional sparse, scattered label present ipsilaterally in the dorsal part of the central nucleus, as well as in tissue lateral to these structures (e.g., Fig. 14; see also Fig. 16). Although the projection to the DC from A-I was bilateral, the ipsilateral projection was more prominent. Patterns of label were similar across three of the four cases, even though slightly different best frequency regions were injected.

Tamarins 87-22, 87-29, and 87-45 had injections of HRP-WGA that were centered in representations in A-I with best frequencies of approximately 10 kHz, 15 kHz, and 9 kHz, respectively. In all three cases, at least two distinct bands of label, oriented dorsomedially to ventrolaterally, were present in the caudal portion of the DC (e.g., Figs. 14, 15, 16). These bands of label became more diffuse and merged into a single band of labeled terminals in more rostral sections (e.g., Figs. 14, 16). In tamarin 87-60, a region of cortex with

neurons responsive to best frequencies around 16 kHz received the HRP-WGA injection. The resulting label formed dorsomedially- to ventrolaterally oriented bands in the ventromedial sector of the DC and did not extend into more dorsolateral portions of the DC, as was seen for the other cases (e.g., Fig. 16; see also Fig. 18).

DISCUSSION

Tonotopic organization and architecture of A-I

A-I of tamarins was characterized by robust neural responses to pure tones and clicks, and by an orderly repre-

Fig. 16. Transported label in the inferior colliculus in a rostral (#167) to caudal (#152) series of frontal sections after an injection of HRP-WGA in A-I in tamarin 87-29. Conventions as in Figure 14.

Projections to the inferior colliculus from A-I

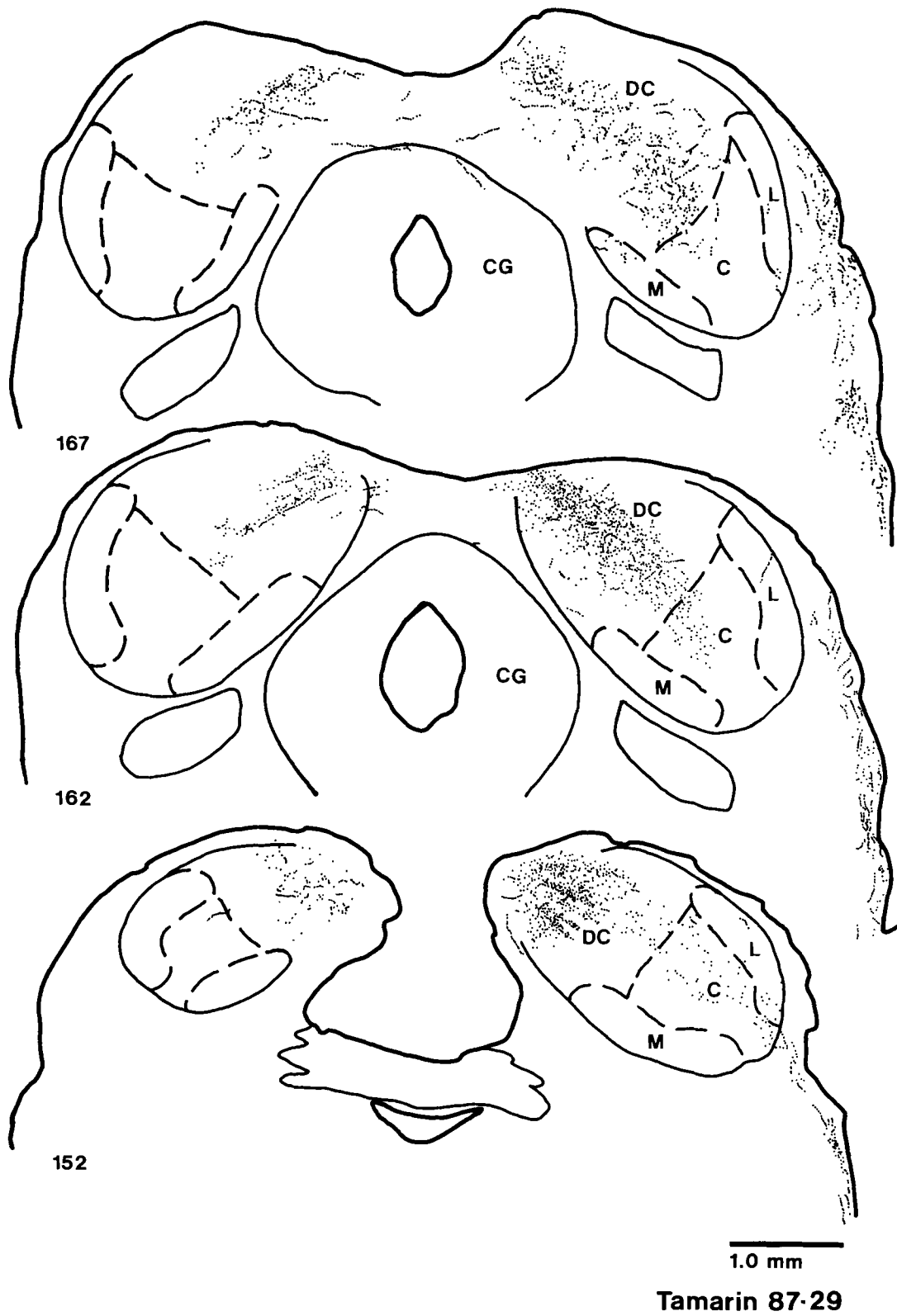


Figure 16

sensation of the frequency spectrum with high frequencies represented caudomedial to low frequencies. Isofrequency contours were oriented approximately perpendicular to the progression of high to low best frequencies within A-I. These physiological findings are in good agreement with those reported for the closely related marmosets by Aitkin et al. ('86), and for other primates (e.g., macaque monkey, Walzl and Woolsey, '43; Merzenich and Brugge, '73; squirrel monkey, Hind et al., '58; chimpanzee, Woolsey, '71; owl monkey, Imig et al., '77; galago, Brugge, '82). In addition, a similar pattern of frequency representation with a range of somewhat different orientations is common to many species of nonprimate mammals (for review see Luethke et al., '88).

The physiologically defined A-I was within a heavily myelinated oval of cortex as seen in cortical sections cut parallel to the surface (also see Krubitzer and Kaas, '86; Luethke et al., '88). In more standard preparations, Merzenich and Brugge ('73) described A-I of macaque monkeys as being densely populated with small cells in layers II-IV (i.e., auditory koniocortex), and Sanides ('72) showed that auditory koniocortex of monkeys is densely myelinated. Similar cytoarchitectonic features have been described for A-I in a variety of mammals (e.g., Oliver et al., '76; Imig et al., '77; Gates and Aitkin, '82; Kraus and Disterhoft, '82; Brugge and Reale, '85; Luethke et al., '88). Based on physiological and architectonic similarities, as well as common connections with the principal or ventral division of the medial geniculate complex (see below), it appears that the same cortical area has been identified as A-I across these species.

Intrinsic connections of A-I

The flattened, surface view preparation used in the present study revealed surface-view patterns of intrinsic connections in A-I. The major horizontal intrinsic connections of A-I were along the isofrequency contours. The smallest injection sites (i.e., rhodamine and diaminidino yellow) labeled neurons along the isofrequency contour of the injection (e.g., Figs. 3, 4, 8). The larger injections (e.g., fast blue and HRP-WGA) produced both bands of label along the isofrequency contours, and more distant and scattered foci of label (Figs. 5, 6, 8). Such patterns of intrinsic connections of A-I have not yet been reported for other primates. However, small injections of HRP in A-I of cats produced bands of label distributed along the isofrequency contour of the injection site, and additional, less dense foci of label outside of the isofrequency contour (Reale et al., '83; Matsubara and Phillips, '88). The similarity of findings in tamarins and in cats suggests that preferential interconnections along the isofrequency contours of A-I is a common feature in mammals.

The less dense foci of label scattered throughout A-I following relatively large injections of tracers, demonstrate interconnections between portions of A-I devoted to different frequencies. Whereas the connections along the isofrequency contours clearly conform to the common observation that neurons with similar physiological properties are often interconnected, the significance of interconnections between neurons mismatched for best frequency is not known. Possibly, the interconnected neurons have other response properties in common. However, Matsubara and Phillips ('88) found no relation between the binaural response properties of the region receiving the injection and the labeled regions in A-I of cats.

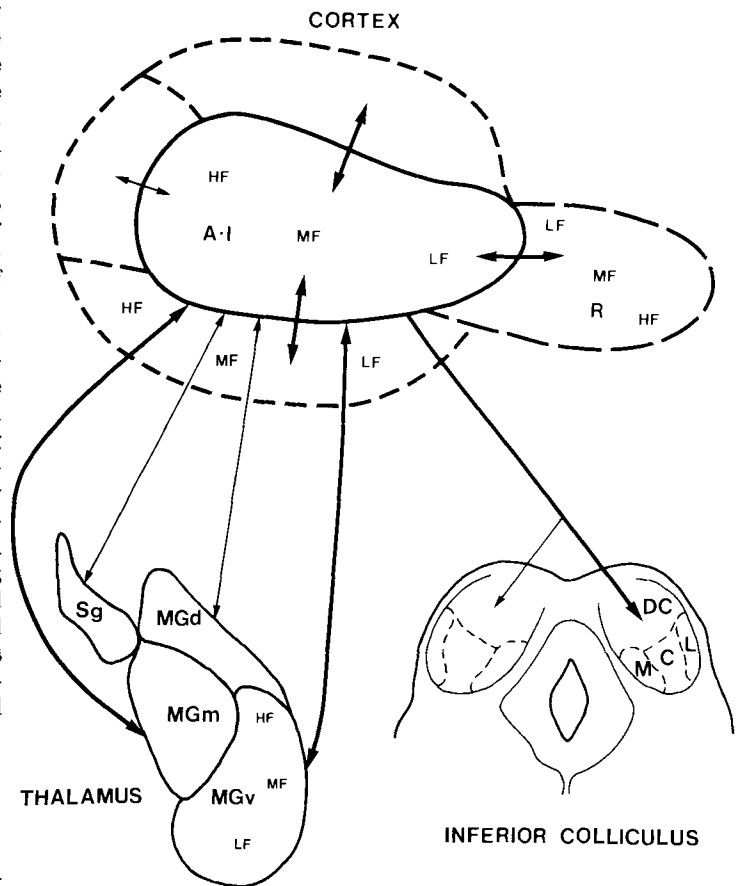


Fig. 17. Summary of the cortical and subcortical connections of A-I (excluding contralateral cortical connections). Heavy arrows indicate dense connections, lighter arrows indicate less dense connections. Dashed lines indicate relatively indistinct architectonic borders. HF, LF, MF, high, low and middle best frequency regions, defined by physiological recordings (in A-I) and inferred by connections with known best frequency regions in A-I. Other abbreviations as in previous figures.

Interhemispheric connections of A-I

In tamarins, the contralateral cortical connections of A-I were almost exclusively with A-I (e.g., Figs. 7, 8). Indeed, studies in a variety of mammals, including other primates, have shown that the predominant callosal connections of A-I are with A-I (e.g., Pandya et al., '69; FitzPatrick and Imig, '80; Imig and Reale, '80; Code and Winer, '86; Aitkin et al., '88; Luethke et al., '88). In addition, each injection in A-I resulted in a dense band of label in the contralateral A-I oriented approximately parallel to the isofrequency contours and in a location that matched the location of the injection site (e.g., Figs. 7, 8). In a similar manner, injections of anatomical tracers confined to A-I in owl monkeys (FitzPatrick and Imig, '80) and marmosets (Aitkin et al., '88) labeled the region of the contralateral A-I corresponding in location to the portion of A-I that received the injection. Combined anatomical and electrophysiological studies in A-I of cats (e.g., Imig and Brugge, '78; Imig and Reale, '80) and gray squirrels (Luethke et al., '88) have demonstrated

preferential callosal connections of matched best frequency regions. Thus matched best frequency regions of A-I are callosally connected in a variety of mammals. However, injections also produced smaller foci of callosally transported label scattered throughout A-I (e.g., Figs. 7, 8). Thus some callosal connections of A-I are to regions of contralateral A-I that are mismatched for best frequency.

Occasionally, foci of sparse contralateral cortical label were found outside of A-I in tamarins (e.g., see Figs. 7, 8). Callosal connections of A-I with auditory cortex surrounding A-I have been shown to be quite dense and widespread in owl monkeys (FitzPatrick and Imig, '80), but they appear to be much more restricted and sparse in marmosets (Aitkin et al., '88). These apparent species differences, however, could relate to variations in the effectiveness of the transport of tracers. Quite possibly, the denser and more widespread callosal connection patterns of A-I reported for owl monkeys more accurately reflects the actual pattern for New World monkeys. In cats and squirrels, A-I also has widespread callosal connections with areas outside of A-I (e.g., Imig and Reale, '80; Luethke et al., '88).

Ipsilateral cortical connections of A-I

Injections in A-I of tamarins demonstrated interconnections with a 2–3 mm fringe of cortex surrounding A-I. The pattern of these connections suggests that this fringe contains three or four distinct auditory fields (summarized in Fig. 17).

Rostral field, R. The most clearly defined field bordering A-I is the rostral field, R, which is topographically interconnected with A-I, and is more densely myelinated than other auditory fields in the fringe. Based on the common features of position relative to A-I, relatively dense myelination, and a topographic pattern of connections with A-I, R appears to be the same field in tamarins as R or RL in owl monkeys (Imig et al., '77), macaque monkeys (Merzenich and Brugge, '73), and marmosets (Aitkin et al., '86). Whereas the frequency representation in R was determined with microelectrodes in owl (Imig et al., '77) and macaque (Merzenich and Brugge, '73) monkeys, R was difficult to map in marmosets (Aitkin et al., '86) and R was not responsive enough to map in tamarins. The reason for these differences in responsiveness is unclear, but higher order areas may be more susceptible to disruption in the marmoset family. Interestingly, area 1 of somatosensory cortex responds poorly in tamarins and marmosets, but is easily mapped in squirrel, owl, cebus, and macaque monkeys (see Carlson et al., '85).

In tamarins, the connection pattern with A-I suggests that low frequencies are represented caudomedially and high frequencies rostromedially in R (Fig. 17). Although there is a reversal in best frequency across the common low frequency border of A-I, R appears to be somewhat rotated so that middle frequency portions of R also border low frequency regions of A-I.

Connections between A-I and R have been previously demonstrated in marmosets (Aitkin et al., '88) and owl monkeys (FitzPatrick and Imig, '80). Whereas the single injections in these studies were not optimal for revealing topography, injections placed in different best frequency locations in A-I in marmosets resulted in different locations of transported label in the field rostral to A-I in a pattern suggesting a reversal of best frequency across the border of A-I with R (Aitkin et al., '88). In the report of FitzPatrick

and Imig ('80), injection sites varied little in location, but results were consistent with the view that A-I is topographically interconnected with R.

Other fields. Patterns of connections suggest the existence of as many as three fields in addition to R in the auditory belt around A-I. A cortical field with apparent topographic connections with A-I was located lateral or caudolateral to A-I (Fig. 17). Injections of multiple tracers in different frequency representations in A-I revealed a largely parallel pattern of connections of A-I with this lateral field. However, multiple foci of label were often seen in the lateral region following a single injection of tracer in A-I (e.g., Figs. 6, 8). This was especially true following HRP-WGA injections (e.g., Figs. 6, 8). Perhaps the multiple foci of label reflect connections that are mismatched for tonotopic locations, or possibly the lateral field has a more diffuse or more complex tonotopic organization than A-I, perhaps with repeating regions of the same best frequency. Evidence from a case in which a larger range of best frequency regions of A-I received clearly separated injections (tamarin 87-22, Fig. 5) revealed the most obvious pattern of parallel connections with the lateral field. Thus as in A-I, neurons responsive to high frequencies appear to be located caudal or caudolateral to those responsive to lower frequencies in the lateral field. Whereas the border between A-I and the region lateral to A-I in tamarins is distinct myeloarchitectonically, other borders for this lateral field are unclear (e.g., Fig. 4).

By location, the lateral auditory field in tamarins corresponds to the lateral cytoarchitectonic field, L, of macaque monkeys (Merzenich and Brugge, '73) and the posterolateral field, PL, of owl monkeys (Imig et al., '77; FitzPatrick and Imig, '80). Connections between A-I and cortex caudolateral to A-I previously have been found in marmosets (Aitkin et al., '88) and owl monkeys (FitzPatrick and Imig, '80). Although best frequencies were determined for neurons caudolateral to A-I in marmosets, the tonotopic organization of this region was not clear (Aitkin et al., '86). More complete evidence for a field lateral to A-I (L) with a tonotopic organization parallel to that seen in A-I was found in the macaque monkey (Merzenich and Brugge, '73). Present results are consistent with the possibility of a tonotopically organized field lateral or caudolateral to A-I in primates.

A medial region of cortex was interconnected with A-I in what appears to be a largely parallel topographic pattern (e.g., Figs. 5, 6, 8). However, single locations in A-I project to multiple loci within the medial field, suggesting a complex organization and the possibility of more than one field in this region (Fig. 4). The medial field corresponds to the caudomedial field, CM, of macaque (Merzenich and Brugge, '73) and owl monkeys (Imig et al., '77). Details of the frequency organization of CM have not been determined by recording techniques (Merzenich and Brugge, '73; Imig et al., '77; Aitkin et al., '86), but CM receives inputs from A-I in owl monkeys (FitzPatrick and Imig, '80).

Cortex caudal to A-I consistently contained transported HRP-WGA, but rarely contained transported fluorescent tracer (e.g., Figs. 5, 6). Whereas the connections with A-I suggest that this caudal region is auditory, organizational features are unclear. The caudal field is indistinct from the medial field myeloarchitectonically (Fig. 4). A-I has also been shown to have connections with cortex caudal to A-I in marmosets (Aitkin et al., '86; '88), but it is uncertain if this caudal field in tamarins and marmosets corresponds to any of the auditory fields identified in owl or macaque monkeys.

Subcortical connections of A-I

The subcortical connections of A-I are summarized in Figure 17. They include interconnections with several subdivisions of the medial geniculate complex, and projections to the inferior colliculus.

Thalamic connections. By examining adjacent tissue sections stained for Nissl substance, myelin, or cytochrome oxidase, dorsal (MGd), ventral (MGv), and medial (MGm) divisions of the medial geniculate complex could be reliably identified in tamarins. Similar subdivisions have been reported for owl monkeys (FitzPatrick and Imig, '78), macaque monkeys (Burton and Jones, '76), and squirrel monkeys (Jordon, '73; Burton and Jones, '76). Earlier studies regarding subdivisions of the medial geniculate complex are reviewed by Jones ('85).

By placing injections of three different tracers in different physiologically defined best frequency regions in A-I of tamarins, we observed a clear topographic pattern of connections with the MGv in single animals (e.g., Figs. 10, 12) and even in single brain sections. Tracers placed in high frequency regions of A-I labeled the dorsal aspect of the MGv, whereas tracers injected in lower frequency regions resulted in label in progressively more ventral portions of the MGv (e.g., Figs. 10, 12). Bands of label resulting from single injections indicate that isofrequency contours are oriented largely in a lateral to medial direction, with a lateroventral slant (e.g., Figs. 12B, 13A). Whereas connections between A-I and the MGv have been demonstrated in owl monkeys (FitzPatrick and Imig, '78) and in rhesus, pigtailed, and squirrel monkeys (Burton and Jones, '76), these studies were not designed to show the topography of these connections. A recent study in marmosets (Aitkin et al., '88), however, did demonstrate the topographic pattern of connections between A-I and the MG complex by placing injections of HRP-WGA into physiologically defined best frequency regions in A-I. Although the MG complex was not subdivided in the marmoset study, it appears that label was present in both portions of the ventral half (MGv) and the dorsal half (MGm and MGd) of the medial geniculate complex. Furthermore, as in the MGv of tamarins, the topographic pattern of connections between A-I and the ventral half of the medial geniculate complex (MGv) of marmosets indicates that high frequencies are represented dorsomedially and low frequencies ventrolaterally. In addition, in a study of the tonotopic organization of the medial geniculate complex in squirrel monkeys, Gross et al. ('74) showed that the ventral region of the medial geniculate complex (corresponding, presumably, to MGv of the present study) is tonotopically organized, with low frequencies represented ventrolateral to higher frequencies.

The tonotopic organization and the topographic pattern of connections of MGv with A-I have been more extensively studied in cats (e.g., Rose and Woolsey, '49; Aitkin and Webster, '72; Colwell and Merzenich, '75; Andersen et al., '80a; Middlebrooks and Zook, '83; Imig and Morel, '83, '84). The high to low frequency representation is largely in a dorsomedial to ventrolateral progression in the nucleus, although topographic patterns of connections suggest further complications (Imig and Morel, '83).

The present results also indicate that there are reciprocal connections between A-I and both the MGd and the MGm of tamarins. Other studies in monkeys (rhesus, pigtailed and squirrel monkeys, Burton and Jones, '78; owl monkeys, FitzPatrick and Imig, '78; marmosets, Aitkin et al., '88), as well

as in cats (e.g., Colwell and Merzenich, '75; Winer et al., '77; Andersen et al., '80a; Winer, '84; Morel and Imig, '87), have also shown connections between A-I and the medial region of the MG.

The present results and those of Aitkin et al. ('88) suggest that A-I and the MGd are interconnected in tamarins and marmosets. However, there was no evidence for significant connections between A-I and the MGd in owl monkeys (FitzPatrick and Imig, '78) and rhesus, pigtailed, and squirrel monkeys (Burton and Jones, '76). Studies in cats and tree shrews have also failed to find interconnections between A-I and the MGd (e.g., Sousa-Pinto, '73; Casseday et al., '76; Oliver and Hall, '78). In contrast, connections of A-I with MGd have been demonstrated in several additional studies in cats (e.g., Andersen et al., '80a; Imig and Morel, '84; Morel and Imig, '87) and in our study in squirrels (Luethke et al., '88). Overall, some uncertainty remains regarding the question of whether A-I and the MGd are connected in all mammalian species thus far studied. Perhaps the less sensitive tritiated amino acids used as tracers in the studies by FitzPatrick and Imig ('78) and by Burton and Jones ('76) failed to reveal the full extent of the connections between A-I and the MGd in primates. Another possibility is that subdivisions of the medial geniculate complex have been defined differently in the various studies.

Patterns of connections provide evidence for at least crude topographical organizations in the MGd and the MGm. The connections suggest that neurons responsive to high frequencies would tend to be located dorsomedial to neurons responsive to low frequencies in the MGm (e.g., Figs. 10, 12) and neurons activated by high frequencies would be ventrolateral to those related to low frequencies in the MGd (e.g., Fig. 10). Occasionally, the MGm, and to a lesser extent the MGd, contained double-labeled cells. In these cases, double-labeled cells were never observed in the MGv. These findings suggest that whereas the neurons of the MGv project to A-I in a highly specific and systematic manner, neurons of the MGm and MGd project in a more diffuse and less specific manner. Evidence from other studies lend support to this idea. For example, only two morphological types of neurons are found in the MGv (Morest, '64, '65, '71, '75), the MGv is interconnected with only a few cortical fields (e.g., Burton and Jones, '76; Andersen et al., '80a; Morel and Imig, '87), the neural responses recorded in the MGv appear to be purely auditory, and best frequencies are systematically represented (e.g., Lippe and Weinberger, '73a,b; Gross et al., '74; Calford and Webster, '81; Imig and Morel, '85). In contrast, the MGm has at least five classes of neurons with a variety of axonal types (Morest, '64; Winer, '79; Winer and Morest, '83), is connected with a multitude of auditory and nonauditory structures (see Jones, '85, for review), and contains neurons with a range of response properties, including activation by auditory, visual and somatosensory stimuli (e.g., Poggio and Mountcastle, '60; Wepsic, '66). Thus the MGm is involved in more than just auditory function.

The MGd appears to be intermediate in complexity when compared to the MGv and the MGm. That is, the MGd has been described as containing several different kinds of neurons (Winer and Morest, '83), has more restricted connections than the MGm but not as restricted as those of the MGv (see Winer and Morest, '83, for review), more clearly appears to have some tonotopic organization (e.g., Morel and Imig, '87) but also responds to nonauditory input (Lippe and Weinberger, '73a, b). These differences suggest a

fundamentally different role in audition for the MGD than that of the MGv (for further discussion, see Winer and Morest, '83; Winer, '85).

Inferior colliculus. Injections of HRP-WGA in A-I revealed bilateral projections to the inferior colliculus. These terminations were largely restricted to the dorsal cortex (DC) of the inferior colliculus. The ipsilateral projections were denser than the contralateral projections, and single injections produced multiple bands of label in DC (Figs. 14, 16).

Bilateral projections from A-I to the dorsal cortex of the inferior colliculus have been reported previously in monkeys and cats. In owl monkeys, FitzPatrick and Imig ('78) demonstrated dense bilateral projections from A-I to the dorsomedial portion of the inferior colliculus, and scattered sparser terminations in more ventral regions of the inferior colliculus (see Fig. 11 of FitzPatrick and Imig, '78). The region that FitzPatrick and Imig ('78) describe as the dorsomedial region corresponds to the dorsal cortex of the present study. Similar terminations in the inferior colliculus have been reported in cats following injections of tracers in A-I (e.g., Andersen et al., '80b) or following ablation of auditory cortex (e.g., Rasmussen, '64; Morest, '66; Diamond et al., '69; Van Noort, '69; Rockel and Jones, '73a,b; Morest and Oliver, '84). Thus in at least cats and monkeys, A-I projects bilaterally to the dorsal cortex of the inferior colliculus and only slightly, if at all, to the central nucleus of the inferior colliculus.

The present results did not reveal any obvious topographic pattern of projections from A-I to the inferior colliculus. However, only the HRP-WGA injections revealed projections to the inferior colliculus, and thus, few cases were studied. If the tonotopic organization of the tamarin inferior colliculus is similar to that of the squirrel monkey (FitzPatrick, '75), then some of the projections from A-I to the inferior colliculus of tamarins seem to be mismatched for frequencies. In cats, Andersen et al. ('80b) demonstrated that injections of tracers into progressively higher frequency regions of A-I labeled progressively more ventromedial locations in the dorsomedial portion of the inferior colliculus (corresponding to the dorsal cortex of the present study).

In caudal portions of the dorsal cortex of the inferior colliculus, two or more bands of label were present following single injections of HRP-WGA into A-I; these bands merged into a single band in more rostral sectors of the dorsal cortex (e.g., Figs. 14-16). In cats, A-I terminals also distribute in bands in the dorsal portion of the inferior colliculus (Andersen et al., '80b), as do inputs to the central nucleus of the inferior colliculus arising in the lateral nucleus of the superior olivary complex (Schneiderman and Henkel, '87). As may be the case for tamarins, the bands in the central nucleus of cats have the same orientation as the isofrequency contours (Merzenich and Reid, '74; Semple and Aitkin, '79; see Schneiderman and Henkel, '87, for discussion). Since there are several bands, projections from given locations in A-I must relate to several frequencies.

The borders between the subdivisions of the inferior colliculus of the tamarin were based on distinctions in Nissl- and myelin-stained tissue, using subdivisions based on Golgi studies of the cat inferior colliculus (Morest and Oliver, '84; Oliver and Morest, '84). In a physiological study of the inferior colliculus of squirrel monkeys, FitzPatrick ('75) defined a large central nucleus with a single representation of the frequency spectrum, with low frequencies represented dorso-caudolateral to high frequencies. Whereas the tonotopic

organization of the squirrel monkey inferior colliculus argues against the existence of functionally distinct subdivisions within the large central nucleus, the connectional and cytoarchitectonic results in tamarins and in owl monkeys (FitzPatrick and Imig, '78) support the traditional division of the inferior colliculus into a dorsal cortical region and a more ventrally located central nucleus.

ACKNOWLEDGMENTS

We thank Anne Morel, John Wall, Michael Huerta, Preston Garraghty, and Sherre Florence for helpful comments on the manuscript. This research was supported by NIMH predoctoral fellowship F31-MH09588 to L.E.L. and NIH grant NS16446 to J.H.K.

LITERATURE CITED

- Aitkin, L.M., and W.R. Webster (1972) Medial geniculate body of the cat: Organization and responses to tonal stimuli of neurons in ventral division. *J. Neurophysiol.* 35:365-380.
- Aitkin, L.M., M. Kudo, and D.R.F. Irvine (1988) Connections of the primary auditory cortex in the common marmoset, (*Callithrix jacchus*). *J. Comp. Neurol.* 269:235-248.
- Aitkin, L.M., M.M. Merzenich, D.R.F. Irvine, J.C. Clarey, and J.E. Nelson (1986) Frequency representation in auditory cortex of the common marmoset (*Callithrix jacchus*). *J. Comp. Neurol.* 252:175-185.
- Allman, J.M., and J.H. Kaas (1971) A representation of the visual field in the caudal third of the middle temporal gyrus of the owl monkey (*Aotus trivirgatus*). *Brain Res.* 31:85-105.
- Allman, J.M., and J.H. Kaas (1974) A crescent-shaped cortical visual area surrounding the middle temporal area (MT) in the owl monkey (*Aotus trivirgatus*). *Brain Res.* 81:199-213.
- Andersen, R.A., P.L. Knight, and M.M. Merzenich (1980a) The thalamocortical and corticothalamic connections of AI, AII and the anterior auditory field (AAF) in the cat: Evidence for two largely segregated systems of connections. *J. Comp. Neurol.* 194:663-701.
- Andersen, R.A., R.L. Snyder, and M.M. Merzenich (1980b) The topographic organization of cortico-collicular projections from physiologically identified loci in the AI, AII, and anterior auditory cortical fields of the cat. *J. Comp. Neurol.* 191:479-494.
- Brugge, J.F. (1982) Auditory cortical areas in primates. In C.N. Woolsey (ed). *Cortical Sensory Organization: Vol. 3. Multiple Auditory Areas*. Clifton, NJ: Humana Press, pp. 59-70.
- Brugge, J.F., and R.A. Reale (1985) Auditory cortex. In A. Peters and E.G. Jones (eds). *Cerebral Cortex, Vol. 4. Association and Auditory Cortices*. New York: Plenum Press, pp. 229-271.
- Brunso-Bechtold, J.K., G.C. Thompson, and R.B. Masterton (1981) HRP study of the organization of auditory afferents ascending to central nucleus of inferior colliculus in cat. *J. Comp. Neurol.* 197:705-722.
- Burton, H., and E.G. Jones (1976) The posterior thalamic region and its cortical projection in New World and Old World monkeys. *J. Comp. Neurol.* 168:249-302.
- Calford, M.B., and W.R. Webster (1981) Auditory representation within principal division of cat medial geniculate body: An electrophysiological study. *J. Neurophysiol.* 45:1013-1028.
- Carlson, M., M.F. Huerta, C.G. Cusick, and J.H. Kaas (1985) Studies on the evolution of multiple somatosensory representations in primates: The organization of anterior parietal cortex in the New World Callitrichid, *Saguinus*. *J. Comp. Neurol.* 246:409-426.
- Casseday, J.H., I.T. Diamond, and J.K. Harting (1976) Auditory pathways to the cortex in *Tupaia glis*. *J. Comp. Neurol.* 166:303-340.
- Code, R.A., and J.A. Winer (1986) Commissural neurons in layer III of cat primary auditory cortex (AI): Pyramidal and non-pyramidal cell input. *J. Comp. Neurol.* 242: 485-510.
- Colwell, S.A., and M.M. Merzenich (1975) Organization of thalamocortical and corticothalamic projections to and from physiologically defined loci within primary auditory cortex in the cat. *Anat. Rec.* 181:336.
- Conde, F. (1987) Further studies on the use of the fluorescent tracers Fast blue and Diamidino yellow: Effective uptake area and cellular storage sites. *J. Neurosci. Meth.* 21:31-43.
- Diamond, I.T., E.G. Jones, and T.P.S. Powell (1969) The projection of the

- auditory cortex upon the diencephalon and brain stem in the cat. *Brain Res.* 15:305-340.
- FitzPatrick, K.A. (1975) Cellular architecture and topographic organization of the inferior colliculus of the squirrel monkey. *J. Comp. Neurol.* 164:185-208.
- FitzPatrick, K.A., and T.J. Imig (1978) Projections of auditory cortex upon the thalamus and midbrain in the owl monkey. *J. Comp. Neurol.* 177:537-556.
- FitzPatrick, K.A., and T.J. Imig (1980) Auditory cortico-cortical connections in the owl monkey. *J. Comp. Neurol.* 192:589-610.
- Gallyas, F. (1979) Silver staining of myelin by means of physical development. *Neurol. Res.* 1:203-209.
- Gates, G.R., and L.M. Aitkin (1982) Auditory cortex in the marsupial possum, *Trichosurus vulpecula*. *Hearing Res.* 7:1-11.
- Gould, H.J., III, and J.H. Kaas (1981) The distribution of commissural terminations in somatosensory areas I and II of the grey squirrel. *J. Comp. Neurol.* 196:489-504.
- Gross, N.B., W.S. Lifschitz, and D.J. Anderson (1974) The tonotopic organization of the auditory thalamus of the squirrel monkey, (*Saimiri sciureus*). *Brain Res.* 65:323-332.
- Hind, J.E., R.M. Benjamin, and C.N. Woolsey (1958) Auditory cortex of the squirrel monkey (*Saimiri sciureus*). *Fed. Proc. Fed. of Amer. Soc. Exp. Biol.* 17:71.
- Imig, T.J., and J.F. Brugge (1978) Sources and terminations of callosal axons related to binaural and frequency maps in primary auditory cortex of the cat. *J. Comp. Neurol.* 182:637-660.
- Imig, T.J., and A. Morel (1983) Organization of the thalamocortical auditory system in the cat. *Ann. Rev. Neurosci.* 6:95-120.
- Imig, T.J., and A. Morel (1984) Topographic and cytoarchitectonic organization of thalamic neurons related to their targets in low-, middle-, and high-frequency representations in cat auditory cortex. *J. Comp. Neurol.* 227:511-539.
- Imig, T.J., and A. Morel (1985) Tonotopic organization in the ventral nucleus of the medial geniculate body in the cat. *J. Neurophysiol.* 53:309-340.
- Imig, T.J., and R.A. Reale (1980) Patterns of cortico-cortical connections related to tonotopic maps in cat auditory cortex. *J. Comp. Neurol.* 192:293-332.
- Imig, T.J., M.A. Ruggero, L.M. Kitzes, E. Javel, and J. Brugge (1977) Organization of auditory cortex in the owl monkey (*Aotus trivirgatus*). *J. Comp. Neurol.* 171:111-128.
- Jones, E.G. (1985) *The Thalamus*. New York: Plenum Press.
- Jordan, H. (1973) The structure of the medial geniculate nucleus (MGN): A cyto- and myeloarchitectonic study in the squirrel monkey. *J. Comp. Neurol.* 148:469-480.
- Kraus, N., and J.F. Disterhoft (1982) Response plasticity of single neurons in rabbit auditory association cortex during tone-signal learning. *Brain Res.* 246:205-215.
- Krubitzer, L.A., and J.H. Kaas (1986) The second somatosensory area in primates: Somatotopic organization, architecture, and connections in marmosets (*Callithrix jacchus*). *Soc. Neurosci. Abstr.* 12:798.
- Kudo, M. (1981) Projections of the nuclei of the lateral lemniscus in the cat: An autoradiographic study. *Brain Res.* 221:57-69.
- Lippe, W.R., and N.M. Weinberger (1973a) The distribution of click evoked activity within the medial geniculate body of the anesthetized cat. *Exp. Neurol.* 39:507-523.
- Lippe, W.R., and N.M. Weinberger (1973b) The distribution of sensory evoked activity within the medial geniculate body of the anesthetized cat. *Exp. Neurol.* 40:431-444.
- Luethke, L.E., L.A. Krubitzer, and J.H. Kaas (1987) Connections of primary auditory cortex in primates. *Soc. Neurosci. Abstr.* 13:327.
- Luethke, L.E., L.A. Krubitzer, and J.H. Kaas (1988) Cortical connections of electrophysiologically and architectonically defined subdivisions of auditory cortex in squirrels. *J. Comp. Neurol.* 268:181-203.
- Matsubara, J.A., and D.P. Phillips (1988) Intracortical connections and their physiological correlates in the primary auditory cortex (AI) of the cat. *J. Comp. Neurol.* 268:38-48.
- Merzenich, M.M., and J.F. Brugge (1973) Representation of the cochlear partition on the superior temporal plane of the macaque monkey. *Brain Res.* 50:275-296.
- Merzenich, M.M., and M.D. Reid (1974) Representation of the cochlea within the inferior colliculus of the cat. *Brain Res.* 77:397-415.
- Mesulam, M.M. (1978) Tetramethylbenzidine for horseradish peroxidase neurohistochemistry: A non-carcinogenic blue reaction product with superior sensitivity for visualizing neural afferents and efferents. *J. Histochem. Cytochem.* 26:160-177.
- Middlebrooks, J.C., and J.M. Zook (1983) Intrinsic organization of the cat's medial geniculate body identified by projections to binaural response-specific bands in the primary auditory cortex. *J. Neurosci.* 3:203-224.
- Morel, A., and T.J. Imig (1987) Thalamic projections to fields A, AI, P, and VP in the cat auditory cortex. *J. Comp. Neurol.* 265:119-144.
- Morest, D.K. (1964) The neuronal architecture of the medial geniculate body of the cat. *J. Anat., Lond.* 98:611-630.
- Morest, D.K. (1965) The laminar structure of the medial geniculate body of the cat. *J. Anat., Lond.* 99:143-160.
- Morest, D.K. (1966) The non-cortical neuronal architecture of the inferior colliculus of the cat. *Anat. Rec.* 154:477.
- Morest, D.K. (1971) Dendrodendritic synapses of cells that have axons: The fine structure of the Golgi type II cell in the medial geniculate body of the cat. *Z. Anat. Entwickl.-Gesch.* 133:216-246.
- Morest, D.K. (1975) Synaptic relationships of Golgi type II cells in the medial geniculate body of the cat. *J. Comp. Neurol.* 162:157-193.
- Morest, D.K., and D.L. Oliver (1984) The neuronal architecture of the inferior colliculus in the cat: Defining the functional anatomy of the auditory midbrain. *J. Comp. Neurol.* 222:209-236.
- Oliver, D.L., and W.C. Hall (1978) The medial geniculate body of the tree shrew, *Tupaia glis* II. Connections with the neocortex. *J. Comp. Neurol.* 182:459-494.
- Oliver, D.L., and D.K. Morest (1984) The central nucleus of the inferior colliculus in the cat. *J. Comp. Neurol.* 222:237-264.
- Oliver, D.L., M.M. Merzenich, G.L. Roth, W.C. Hall, and J.H. Kaas (1976) Tonotopic organization and connections of primary auditory cortex in the tree shrew, *Tupaia glis*. *Anat. Rec.* 184:491.
- Osen, K.K. (1972) Projection of the cochlear nuclei on the inferior colliculus in the cat. *J. Comp. Neurol.* 144:355-372.
- Pandya, D.N., M. Hallett, and S.K. Mukherjee (1969) Intra- and interhemispheric connections of the neocortical auditory system in the rhesus monkey. *Brain Res.* 14:49-65.
- Poggio, G.F., and V.B. Mountcastle (1960) A study of the functional contributions of the lemniscal and spinothalamic systems to somatic sensibility: Central nervous mechanisms in pain. *Bull. Johns Hopkins Hosp.* 106:266-316.
- Rasmussen, G.L. (1964) Anatomical relationships of the ascending and descending auditory systems. In W.S. Field and B.R. Alford (eds). *Neurological Aspects of Auditory and Vestibular Disorders*. Springfield, IL: Thomas, pp. 5-23.
- Reale, R.A., J.F. Brugge, and J.Z. Feng (1983) Geometry and orientation of neuronal processes in cat primary auditory cortex (AI) related to characteristic-frequency maps. *Proc. Natl. Acad. Sci.* 80:5449-5453.
- Rockel, A.J., and E.G. Jones (1973a) The neuronal organization of the inferior colliculus of the adult cat. I. The central nucleus. *J. Comp. Neurol.* 147:11-60.
- Rockel, A.J., and E.G. Jones (1973b) The neuronal organization of the inferior colliculus of the adult cat. II. The pericentral nucleus. *J. Comp. Neurol.* 149:301-334.
- Rose, J.E., and C.N. Woolsey (1949) Organization of the mammalian thalamus and its relationships to the cerebral cortex. *Electroencephalogr. Clin. Neurophysiol.* 1:391-403.
- Roth, G.L., L.M. Aitkin, R.A. Andersen, and M.M. Merzenich (1978) Some features of the spatial organization of the central nucleus of the inferior colliculus of the cat. *J. Comp. Neurol.* 182:661-680.
- Sanides, F. (1972) Representation in the cerebral cortex and its areal lamination patterns. In G.H. Bourne (ed): *The Structure and Function of Nervous Tissue*, Vol. 5. New York: Academic Press, pp. 330-449.
- Schneiderman, A., and C.K. Henkel (1987) Banding of lateral superior olivary nucleus afferents in the inferior colliculus: A possible substrate for sensory integration. *J. Comp. Neurol.* 266:519-534.
- Semple, M.N., and L.M. Aitkin (1979) Representation of sound frequency and laterality by units in the central nucleus of cat inferior colliculus. *J. Neurophysiol.* 42:1626-1639.
- Shook, B.L., B.P. Abramson, and L.M. Chalupa (1984) An analysis of the transport of WGA-HRP in the cat's visual system. *J. Neurosci. Meth.* 11:65-77.
- Sousa-Pinto, A. (1973) Cortical projections of the medial geniculate body in the cat. *Ergeb. Anat. Entwicklungsgesch.* 48:1-40.
- Thanos, S., and F. Bonhoeffer (1983) Investigations on the development and topographic order of retinotectal axons: Anterograde and retrograde staining of axons and perikarya with rhodamine in vivo. *J. Comp. Neurol.* 219:420-430.
- Thanos, S., and F. Bonhoeffer (1984) Development of the transient ipsilateral retinotectal projection in the chick embryo: A numerical fluorescence-

- microscopic analysis. *J. Comp. Neurol.* 224:407-414.
- Thanos, S., M. Vidal-Sanz, and A.J. Aguayo (1987) The use of rhodamine-isothiocyanate (RITC) as an anterograde and retrograde tracer in the adult rat visual system. *Brain Res.* 406:317-321.
- Van Noort, J. (1969) The Structure and Connections of the Inferior Colliculus. An Investigation of the Lower Auditory System. Assen: Van Gorcum.
- Walzl, E.M., and C.N. Woosley (1943) Cortical auditory areas of the monkey as determined by electrical excitation of nerve fibers in the osseous spiral lamina and by click stimulation. *Fed. Proc. Fed. Amer. Soc. Exp. Biol.* 2:52.
- Wepsic, J.G. (1966) Multimodal sensory activation of cells in the magnocellular medial geniculate nucleus. *Exp. Neurol.* 15:299-318.
- White, P.F., W.L. Way, and A.J. Trevor (1982) Ketamine—its pharmacology and therapeutic uses. *Anesthesiology* 56:119-136.
- Winer, J.A. (1979) Neurons in the medial division of the medial geniculate body of the cat. *Anat. Rec.* 193:723.
- Winer, J.A. (1984) Identification and structure of neurons in the medial geniculate body projecting to primary auditory cortex (AI) in the cat. *Neurosci.* 13:395-413.
- Winer, J.A. (1985) The medial geniculate body of the cat. *Anat. Embryol.* 86:1-97.
- Winer, J.A., and D.K. Morest (1983) The neuronal architecture of the dorsal division of the medial geniculate body of the cat. A study with the rapid Golgi method. *J. Comp. Neurol.* 221:1-30.
- Winer, J.A., I.T. Diamond, and D. Raczkowski (1977) Subdivisions of the auditory cortex of the cat: The retrograde transport of horseradish peroxidase to the medial geniculate body and posterior thalamic nuclei. *J. Comp. Neurol.* 176:387-418.
- Wong-Riley, M. (1979) Changes in the visual system of monocularly sutured or enucleated cats demonstrable with cytochrome oxidase histochemistry. *Brain Res.* 171:11-28.
- Woolsey, C.N. (1971) Tonotopic organization of the auditory cortex. In M.B. Sachs (ed): *Physiology of the Auditory System*. Baltimore: National Educational Consultants, pp. 271-282.